

Development Of Autonomous Weighing System for Southern Ground Hornbill



Prepared by:

Zaccary Beilinson, Ethan Morris, Devlin Trafford, Tinotenda Togara

Prepared for:

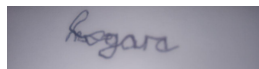
EEE4113F

Department of Electrical Engineering
University of Cape Town

June 1, 2024

Declaration

1. I know that plagiarism is wrong. Plagiarism is to use another's work and pretend that it is one's own.
2. I have used the IEEE convention for citation and referencing. Each contribution to, and quotation in, this report from the work(s) of other people has been attributed, and has been cited and referenced.
3. This report is my own work.
4. I have not allowed, and will not allow, anyone to copy my work with the intention of passing it off as their own work or part thereof.



Contents

1	Introduction	1
1.0.1	Proposed Solution	1
1.0.2	Scope and Limitations	1
1.0.3	Report Breakdown	2
2	Literature Review	3
2.1	Introduction	3
2.2	General Wildlife Monitoring	3
2.2.1	Acoustic Source Detection	3
2.2.2	RFID Technology	4
2.2.3	Camera Traps	4
2.2.4	Wireless Sensor Networks	4
2.2.5	Concluding remarks	5
2.3	Southern Ground Hornbill	5
2.3.1	About the Southern Ground Hornbill	5
2.3.2	Endangered status	5
2.3.3	Monitoring and preservation	6
2.4	Weighing techniques for wild birds	7
2.5	Hardware	7
2.5.1	Power supply	7
2.5.2	Camera trap	8
2.6	Conclusion	9
3	Sensing	11
3.1	Introduction	11
3.2	Specifications and requirements	11
3.2.1	System Requirements	11
3.2.2	Functional Specifications	11
3.3	Design Choices	12
3.4	Prototype design	15
3.5	Acceptance Test Procedures (ATPs)	15
3.5.1	Individual Load Cell Testing	15
3.5.2	Combined Load Cell Testing	19
3.5.3	Temperature Sensor Testing	21
3.5.4	Camera Testing	21
3.6	Conclusion	22

4	Processing Hardware and Device Enclosure	23
4.1	Introduction	23
4.1.1	Functional and Technical Requirements	23
4.2	Theory	24
4.2.1	Enclosure Ratings	24
4.3	Design Choices	25
4.4	Final Design	30
4.5	Acceptance Test Procedures	31
4.6	Discussion of Test Results	32
4.7	Conclusion	33
5	Data Processing	34
5.1	Introduction	34
5.2	Design Process & Design Choices	35
5.2.1	Design Process	35
5.2.2	Design Choices	38
5.2.3	Acceptance Test Procedures	38
5.3	Final Design	39
5.3.1	Data Acquisition	39
5.3.2	Pre-processing	40
5.3.3	Filtering	40
5.3.4	Storage	40
5.4	Testing & Results	43
5.5	Conclusion	45
6	Power Subsystem	46
6.1	Introduction	46
6.2	Design Choices	46
6.2.1	Batteries	46
6.2.2	Buck Converters	47
6.2.3	Solar-Based System Components	49
6.3	FINAL DESIGN	50
6.3.1	LM317 Integrated Circuit	51
6.4	POWER BUDGET	51
6.4.1	Active Mode	51
6.4.2	Sleep mode	51
6.5	TESTING/RESULTS	52
6.6	CONCLUSION	52
7	Conclusions	53
8	Recommendations	54
	Bibliography	55

Chapter 1

Introduction

Dr. Mark-Middleton and Carrie Hickman, two wildlife conservationists working for the Associated Private Nature Reserves (APNR) ground hornbill project, need a way to autonomously weigh and record weight data for Southern Ground Hornbills (SGH) because interestingly in their world they have to watch kitchen scales with binoculars in order to manually record this data.

This approach has many downsides. Southern Ground Hornbills are very skittish and typically avoid interaction with humans. This means that recording these measurements relies on luck and timing since the bird has to land on the scale while they are observing it and for long enough to obtain a reading. Additionally birds do not remain still on these scales, which causes lots of fluctuation in the scale readings. As a result the recordings depend on human interpretation and are at best rough estimates of the true value. The issue is clear: large amounts of time and labour are being funnelled into an approach with no guarantee of data and in instances where data is obtained it is inaccurate and subject to human error.

1.0.1 Proposed Solution

These problems provide room for a solution in the form of an autonomous scale system. The benefits of an autonomous system are plural: it reduces the frequency of site visits as well as the time spent by the stakeholders at the site. This in turn reduces the potential for skewed data and minimises the labour and time costs associated with the current methods. In addition to this, the implementation of digital sensors and a suitable filtering algorithm allows for a much higher degree of accuracy when measuring and recording data.

1.0.2 Scope and Limitations

Scope

This report focuses on the design and development of an autonomous scale system, encompassing hardware and software components. It involves integrating weight and temperature sensors, implementing a data filtering algorithm for improved accuracy, and conducting testing to ensure functionality and performance align with objectives. The report also highlights the system's suitability for specific environments, namely the Kruger region. Consideration is given to relevant metrics throughout the report.

Limitations

The report does not explore the suitability or performance of the automatic scale system in low-weight fine accuracy applications. The report does not investigate the effectiveness or challenges of deploying the automatic scale system in sub-zero environments, which could impact its functionality. The report's findings are influenced by time limitations which affect the depth of research, data collection, and analysis. The report faced limitations in accessing specialized material testing facilities to evaluate the compatibility and durability of the automatic scale system components. The report was constrained by difficulties in obtaining sufficient access to Southern Ground Hornbills for conducting real-world testing of the automatic scale system's performance and interactions.

1.0.3 Report Breakdown

This report presents a comprehensive breakdown of a multidisciplinary project focused on the integration of four key sections: sensing, power, software, and hardware. The project aims to develop a sophisticated system that combines sensing capabilities, efficient power management, robust software solutions, and reliable hardware components. To provide a solid foundation for the project, an extensive literature review is conducted, exploring relevant research and technological advancements pertaining to each project section. This review serves as a basis for understanding the current state of the field and identifying potential gaps and challenges. The subsequent sections of the report delve into the requirements, specifications, design process, final prototypes, test procedures, and results for each respective section, offering a comprehensive analysis of the project's progress. Furthermore, future recommendations are provided to guide further advancements and enhancements in the integrated system. The sub-systems were distributed as follows:

Sensing - Devlin Trafford

Processing Hardware and Device Enclosure - Zaccary Beilinson

Data Processing - Ethan Morris

Power Subsystem - Tinotenda Togara

Chapter 2

Literature Review

2.1 Introduction

This chapter provides a comprehensive review of the various elements of literature pertaining to wildlife monitoring, with a specific focus on the Southern Ground Hornbill. The review commences with an examination of previous systems for monitoring wildlife, followed by an exploration of conservation efforts and current monitoring techniques surrounding the Southern Ground Hornbill.

Furthermore, an analysis of literature that specifically focuses on the hardware elements involved in these monitoring systems, including camera traps and battery systems, is provided. This is followed by an in-depth analysis of weighing systems in previous scientific studies. The chapter concludes with a summary of the current state of automated weighing systems.

2.2 General Wildlife Monitoring

This section provides a review of important literature regarding the techniques commonly used in the field of wildlife monitoring. Specific literature highlighting Acoustic Source detection, RFID Technology, Camera Traps and Wireless Sensor Networks is discussed. Notably, while the continued development of software and hardware resources has resulted in the wide-scale adoption of automation within the field, it has similarly given rise to new challenges. These limitations are explored below.

2.2.1 Acoustic Source Detection

The exhibited call and response behaviours of animals have been captured by observers to reproduce it in order to attract and detect wildlife. In the past, this has been undertaken manually, requiring the presence of the researcher in broadcasting a call and recording the received response. In a 2011 article published in the *Wildlife Society Bulletin*, the authors, Ausband et. al, detail issues with manual implementation of Acoustic source detection arising from the need for human presence, which resulted in significant labour intensity and disturbance of animal behaviour thus skewing surveys. [1] Additionally, the rate of detection was found to be a function of the observer's hearing and the capability of their recording equipment. Automated Acoustic sensors serve to increase sampling effort thus increasing the scale and efficacy of monitoring. [2] In a case study conducted in 2010 on the comparability of manual inland audio-visual detection and automated acoustic monitoring for marbled murrelets, it was noted that the number of successful acoustic detections was strongly correlated

with audio-visual detection. Moreover, using automated monitoring facilitated the acquisition of an additional 10 mornings' worth of data per observation site, at a cost that was commensurate with that of audio-visual monitoring. [2]

2.2.2 RFID Technology

With the advent of increasing sensor network integration in wildlife monitoring, a consistent boundary has arisen in the need to make these sensors more sustainable and easier to manage within various deployment environments. Markedly - in an article published in 2010 detailing the deployment of a sensor network to track European badgers residing in a dense woodland area – it was noted that GPS receivers function poorly in wooded areas and would be labour intensive and expensive whilst Very High Frequency (VHF) telemetry would be impractical for large scale animal tracking. [3] Consequently, an RFID system was implemented consisting of RFID transmitters attached to the badgers as wearable collars. This method of monitoring is frequently used across various species with dependency of its use being a result of the locality of species grouping. This results from the fact that a separate collection of detection nodes must be distributed in nearby regions to allow for detection. [3]

2.2.3 Camera Traps

In monitoring terrestrial vertebrate wildlife, Zwerts et al. noted that the selection of monitoring technique should be determined as a function of target species, population metrics under review, expertise and tools required for species identification and financial and human resources available. [4] Camera traps have been used extensively in monitoring rare nocturnal animals alongside those living in extended home ranges or highly sensitive to the presence of humans. [5] To this end, use of camera trapping is prevalent in detection of ground dwelling mammals and birds alongside shy species and is suitable to assess whole communities. [4] The selection of camera trap model alongside the sampling protocol used is essential to successful monitoring of specific target species. The effective selection of camera trap requires the consideration of certain performance characteristics including trigger speed, detection zone (zone covered by camera's infrared beam wherein movement is detected), field of view, night time picture quality and recovery time (time taken before the next picture can be captured) [5] In addition to this, characteristics such as battery consumption and camera cost need to be accounted for. Camera traps cover a small surface area of around 10m² to 20m² and thus placement strategy needs to be carefully considered. Efficacy of camera traps in boosting detection has been shown to be elevated by spacing cameras in relation to trails and streams alongside other areas known to be frequented. [4] These traps are often assisted by lures or bait placed to draw the target species towards them.

2.2.4 Wireless Sensor Networks

In a case study published in 2009, Handcock et al. discuss the implementation of a wireless sensor network in monitoring behavioural preferences and social behaviour of cattle. Handcock brings to light the complications that arise in monitoring animal movement concurrently with landscape condition – as landscape conditions are deemed to affect animal behaviour. [6] This case study saw the deployment of a Wireless Sensor Network (WSN) consisting of an array of nodes – each containing multiple sensors to measure environmental parameters (including soil moisture and micro-climate). The scope of WSN deployments spans a wide array of physical implementation. In effect, a WSN implementation comprises

a collection of sensors each with their own power supply, wireless communication, data storage and data processing capability. Networks of Embedded devices work together to collect and transmit data from remote field sites back to a central base through the use of a gateway node. [6]

2.2.5 Concluding remarks

The continued development in a wide variety of deployed wildlife monitoring techniques has, largely, been steered by ever increasing access to more suitable hardware and software for automation. Whilst this development in monitoring techniques inline with automation offers many benefits to the field - including reducing labour intensity, increasing sampling effort, reducing error in measurement due to human inaccuracies etc. – the literature evidently depicts limitations present as to the extent automation can be used. These limitations arise as a result of challenges concerning the need for maintenance as well as the fiscal investment required to set-up automated systems.

2.3 Southern Ground Hornbill

2.3.1 About the Southern Ground Hornbill

The Southern Ground Hornbill (SGH) is the largest species of Hornbill in the world, characterized by an average weight range of 3 to 4 kilograms and a height ranging from 90 to 110 centimeters when fully grown [7]. These morphological features make the SGH an important and distinct member of the avian fauna of southern Africa, with significant implications for the conservation efforts aimed at preserving the species and its habitat.

Being terrestrial birds, SGHs are known to spend approximately 70% of their diurnal activity foraging in groups on the ground. However, during the night, SGHs typically take refuge in tall trees for roosting in order to avoid potential nocturnal predators[17]. They are found across Southern Africa and occupy areas in Angola, Botswana, Congo, Swaziland, Tanzania and South Africa with the largest population being found in the Kruger National Park. Suitable habitats for SGHs include grassland, savannah and woodland biomes [7].

SGHs have five distinct calls which have been linked to various behaviors in the birds. The most notable of these is a loud booming call to communicate over long-distances and is used to indicate territories. In a 1976 study done by M. Kemp [8] playback of their territorial call was successfully used to attract these birds to areas of interest within their territories.

2.3.2 Endangered status

SGHs are considered vulnerable by the International Union for Conservation of Nature (IUCN) [9], however, due to the declining populations outside of protected areas they have been declared an endangered species in South Africa. The reasons for their falling numbers are wide ranging and include the loss or mutation of suitable habitats, poisoning, mistreatment by humans and electrocution [9].

Another contributing factor to the vulnerability of this species is their unusual mating habits and long fledging periods. SGHs exhibit a mating habit known as cooperative breeding. This involves a group

of birds comprising one dominant mating couple and at least two other helper birds, who serve to forage and protect the dominant pair. Although between 1 and 3 eggs can be laid each breeding season, sibling chicks will fight and kill each other ensuring that only one chick reaches its fledgling stage [7]. In addition, SGHs are slow to mature and have an extended fledging period: groups on average will fledge only one chick every six to nine years [10]. Environmental changes which affect their livelihood and breeding patterns as well as their slow recovery from such changes makes them highly susceptible to population decline.

2.3.3 Monitoring and preservation

The decline in SGH numbers has led to the implementation of various conservation projects in Southern Africa. By collecting data on the birds' movements, habitat and population size, researchers can gain a better understanding of the threats facing the species and develop conservation strategies to protect it. A combination of the below techniques are typically used and combined to form a broad picture of the challenges this species experience.

Visual and auditory surveys: These involve searching for SGHs in their natural habitat and recording their calls and other vocalizations. Surveyors use binoculars, telescopes, or spotting scopes to observe the birds from a distance[11].

Satellite telemetry: This involves attaching a satellite tracking device to the bird and monitoring its movements using GPS technology. This method provides detailed information on the bird's movements and habitat over time.[12]

Radio telemetry: This involves attaching a radio transmitter to a SGHs and tracking its movements using a radio receiver. This method allows researchers to locate the bird in real-time and track its movements over short distances[13].

Nest monitoring: This involves monitoring SGHs' nests to track breeding success and estimate population size. Nest monitoring may involve visual surveys or the use of camera traps to capture images of the birds[14].

Citizen science: This involves enlisting members of the public to report sightings of SGHs and other wildlife. Citizen science projects may use online platforms or mobile apps to collect data from volunteers.

Monitoring the weights of SGHs forms an important part of their overall health assessment. Weight loss or gain can be an early sign of illness or other issues that may require veterinary attention. In captive breeding programs the birds are trained, through positive reinforcement training, to step onto a scale. Once comfortable with stepping onto the scale, the keeper can record their weight by noting the reading on the scale.

Monitoring the weights of wild SGHs can be more challenging than that of captive birds. In general, these birds are skittish and may be resistant to human interaction, which makes their regular capturing and weighing difficult and ultimately unfeasible.

One common method for monitoring the weights of wild SGHs is to use baited weighing scales. Researchers or conservationists can set up a scale near a food source, such as a carcass, and wait for the birds to come and feed. When a bird steps onto the scale to feed, its weight can be observed through

binoculars and recorded by field researchers[10].

2.4 Weighing techniques for wild birds

Wild birds are skittish and often resistant to human contact which makes it difficult to capture them for manual weighing at regular intervals. They are also hyper vigilant animals, which may lead to their detection and avoidance of poorly disguised weight measurement systems and could potentially result in biased, innacurate data collection.

Climate needs to be accounted for when choosing how to disguise the weighing system. A study conducted in 2003 which investigated an automated weighing system for penguins made use of a weighbridge, an electronic tag reader, a direction of motion detector and a controller which logged the recorded data. The weighbridge was populated with static loads used to calibrate and disguise the platform. To test the system, a group of penguins with known weights were allowed to cross the platform. The measurements were shown to have an accuracy of $\pm 5\%$ with a worst case error of 15%. [15]

A journal article written by A. Poole and J. Shoukimas explored an alternative method of weighing birds in their natural habitat. The article details the design of a small, waterproof, low-cost scale, which was disguised as a bird perch and placed inside an aviary. Perching rods were attached to a transducer which was in turn attached to strain gauges. Deflections of the rod changed the voltage seen across the strain gauges which was then used to calculate the birds weight. Temperature fluctuations were found to have little effect on the performance of the transducer, however deviations of as much as $\pm 10\%$ were seen when the strain gauges were subjected to a temperature change of $\pm 15\text{-}20^\circ\text{C}$. [16]

A report written by K. Wang et al. detailed a method for measuring the weight of chickens called the Rod-platform weighing module. The system consists of two rods fixed on each end to an L-shaped bracket which can be adjusted in height. Each L-shaped bracket is connected to a single strain-gauge sensor that is stored in a steel box. Pillars were fixed to the rod to limit the locations where the chickens could settle to reduce uncertainty associated with readings. A microprocessor measured and recorded the output from the two sensors.

The sampling process involved two stages: a peeling and a weighing stage. The peeling stage measured the weight of the empty rod so that its effect could be subtracted from future measurements. The weighing stage then measured and recorded the weight of chickens. Ten samples were taken for each chicken to account for the possibility of movement while perched on the rod. If the difference between any two samples was smaller than the threshold stored in the program, the average of the ten samples was taken to be the stable weight of the chicken.[17]

2.5 Hardware

2.5.1 Power supply

In this section constant power supplies will be explored. The effects of temperature and the presence of water in the vicinity of these supplies will also be explored.

Batteries

A Lithium-ion battery is a rechargeable battery which stores energy using the reversible reduction of lithium ions. In 2010, M. Oswal et al. conducted a comparative study on Lithium-ion batteries. The study went on to mention that a battery is made up of one or more cells, each of which contains three parts: two electrodes and an electrolyte in between them. During the charging process, the cathode withdraws some of its lithium ions which move through the electrolyte to the anode. During the discharging process, the lithium ions move from the anode through the electrolyte back to the cathode. [18] A Lead-acid battery is made up of a pair of electrodes submerged in sulfuric acid. In 2005, H. Bindner et al. noted that each of the electrodes in a lead acid battery is attached to a grid in order to distribute the current and provide the electrode with support mechanically. The charging and discharging processes work similarly to that of the Lithium-ion battery – there is a transfer of ions between the cathode and the anode through the electrolyte[19]. The Lithium-ion battery has a higher energy density due to the material of the electrodes being lithium which is highly reactive – hence more charge can be stored in the same amount of space. [18] An article composed by J Marsh, details that Lithium-ion batteries also have a better depth of discharge. They can discharge 85% of their total capacity without causing long term damage to battery while Lead-acid batteries can only discharge 50% of their capacity without sustaining long term damage. Lithium-ion batteries (90% – 95%) are more battery efficient than Lead-acid batteries (80% - 85%). This metric indicates that the Lithium-ion have a higher effective capacity meaning they can charge at a faster rate. Lithium-ion batteries can last seven times the number of cycles of Lead-acid batteries. [20]The Lithium-ion battery is the better performing battery overall and as a result is the more expensive of the two.

Effects of weather

The need for the battery to function in extreme weather conditions, hot and cold, is discussed in this section. To combat the possibility of contact with water, the batteries available for purchase come pre-packaged in a sealed container – which is designed to both keep the battery elements inside the container and the natural elements outside the container. A 2018 review notes that the temperature effects on the Lithium-ion battery only hamper the performance and lifespan of the battery when the temperature is outside of the optimal working range of the battery which is 15-35°C. Using the battery outside of this range results in a reduction in the efficiency of the charging and discharging processes, and the battery’s overall capacity. [21] A technical report published in 2004 notes that the Lead-acid battery operates at peak performance at a temperature of 25°C and decreases in performance in its overall capacity and rate of charge and discharge as the temperature deviates from that 25°C point. [22]

2.5.2 Camera trap

Camera Traps are used widely used to study animal behaviour and monitor the animals without having to be present at every moment. The camera is set up to take a picture of the desired object at the instant a motion sensor notifies it of a moving object in the area framed by the camera.

Functioning

In 2018, P. J. Apps and J. W. McNutt compiled a report on the workings of a camera trap. They detailed that the motion detector uses heat signatures which recognises a temperature difference of the object relative to that of the surrounding area. The motion detector is made up of between five and seven lenses which all monitor different long, narrow vertical sections of the detection window. Therefore, the motion detector works best when detecting an object moving across the field of view of the camera. [23] The report continues to mention that after the animal crosses from one zone to another, the detector sends a signal to the camera to instruct it to capture an image. The time between the detector sending a signal and the camera capturing a photograph is the trigger delay. [23] F. Trollet et al. noted that after the camera captures an image, recovery time is the time needed before another image can be captured – with different camera models having differing recovery times in the range of 0.5 seconds up to 60 seconds. [5]

Use in Wildlife Monitoring

The use of a camera trap which produces images of a higher resolution would allow for better identification of the object or animal. However, with this increase in resolution the images become heavier to store resulting in a larger storage capacity required for the camera trap to run uninterrupted for an extended period. A scientific journal written by F. Trollet et al. introduced measures that were implemented to ensure the animals are not spooked when the image is captured, such as the use of a flash made of Light Emitting Diodes (LEDs) that emit no visible light and shooting the image in black and white. This process is what creates the effect of an infrared camera. [5] A report written in 2009 by Rössler et al. noted that ultraviolet (UV) rays reflect off the glass of the camera lens and act as an animal deterrent and cause anger in the animal which leads them to damage the lens enough to stop the UV reflection. Solutions explored to solve this issue include the use of marking stickers to prevent the UV reflection and indicate the presence of the glass to the animal [24].

Environmental effects

In their 2018 report, P. J. Apps and J. W. McNutt also wrote about the camera position affects the performance of the motion detector. The difference between the heat signature which needs to be detected, such as animal movement, versus the surrounding area decreases. High temperatures cause another issue in the functioning of the camera trap: if the camera heats up to a temperature which is in the region of the temperatures of the surrounding area, the camera's heat signature will blind the motion detector. The motion detector will then have to wait for the camera to cool down to a lower temperature in order to allow for the motion detector to monitoring the area. This increase in temperature will most likely occur when the camera trap is exposed to direct sunlight or when the temperature of the placement area of the camera is high enough to cause this interference. [23]

2.6 Conclusion

This chapter presents a comprehensive literature review on wildlife monitoring, with a specific focus on the Southern Ground Hornbill. It highlights the limitations of manual weighing techniques, which are often tedious and unfeasible for large populations. An exploration of previous monitoring systems

and conservation efforts for this species is provided, along with an analysis of the hardware elements involved in monitoring systems such as camera traps and battery systems. The in-depth analysis of weighing systems in previous scientific studies lays the groundwork for the discussion of automated weighing systems, which provide a viable solution to the limitations of manual weighing. Integration of an autonomous weighing system with a camera trap offers a promising approach for effective monitoring and management of the Southern Ground Hornbill population.

Chapter 3

Sensing

3.1 Introduction

The primary objective of this project is to aid nature conservation efforts by collecting non-invasive data to improve our understanding of the health and behavioural patterns of SGHs in their natural environment. Sensing circuitry is an integral part of this project, facilitating the accurate capture and recording of the weight, associated temperature and photographic data of the bird.

This section provides an overview of the sensing circuitry, including the components and their functions as well as the design considerations taken into account during the development process. It also outlines the acceptance test procedures designed to evaluate the system's performance, and reports the results of these tests.

3.2 Specifications and requirements

3.2.1 System Requirements

FR-1: The system must measure birds' weights to within 100 grams (a tolerance of 2.5% based on an average bird weight of 4 kilograms.)

FR-2: The system must perform acceptably in temperatures ranging from 0-50°C.

FR-3: The system must be triggered by a threshold weight value.

FR-4: The scale must be equipped with a camera that captures pictures when the threshold weight value is met.

FR-5: The system must account for up to two birds sitting on it simultaneously.

FR-6: The system must take temperature readings and store them with the weight measurements.

FR-7: The temperature sensor must calibrate the weight measurements based on temperature drift.

FR-8: The system must be easily calibrated, and calibration should be simple enough to be done by users with little technical expertise.

FR-9: The camera should be operable in low-light conditions since the birds tend to perch in the early or late hours of the day.

FR-10: The system should be waterproof and durable in high temperature conditions.

3.2.2 Functional Specifications

The functional specifications shown below were derived both from the system requirements shown above and through iterations of the design process.

Table 3.1: Camera

no.	Specification
FS-1	3.3-5V operating voltage
FS-2	Output format 8-bit
FS-3	Sensitivity to low-light conditions
FS-4	Low standby current
FS-5	Operable temperature range 0-50°C

Table 3.2: Temperature Sensor

no.	Specification
FS-6	5V operating voltage
FS-7	<1mW standby power
FS-8	9 bit resolution or better
FS-9	Operable temperature range 0-50°C
FS-10	$\pm 0.5^{\circ}\text{C}$ accuracy or better over 0-50°C temperature range

Table 3.3: Weight Sensor

no.	Specification
FS-11	5V operating voltage
FS-12	Precision better than 0.1%
FS-13	Operable temperature range 0-50°C
FS-14	< 0.1% FS error per 10°C
FS-15	Must be able to measure weights up to 15 kilograms
FS-16	< 0.1% non-linearity error
FS-17	IP65 weather rating

3.3 Design Choices

Load cells were selected as the weight-sensing element as they are simple and reliable, have minimal sensor drift and non-linearity and are cheap. Additionally, amplifying ADC modules specifically designed to interface with them are affordable, there are pre-built arduino libraries for interfacing with them and there are numerous online resources on their use and calibration.

Various different scale configurations were examined in the design process. With many configurations, the bird's position on the scale affected the readings. Initially a tension scale which suspended a perch

from a load cell was considered as the tension applied to the load cell always acts at a constant distance removing the dependence on position. Stakeholder Hickman, however, informed us that the birds would likely not perch on something which could swing freely. Introducing channels to restrict the perch's movement to a vertical axis was considered. This approach was rejected due to the added complexity of the mechanical design and the potential for the perch to lose accuracy due to the friction of the channels. Both of the above problems were solved by introducing a second load cell, with each side of the perch attached to a load cell fastened to branches above the nest. In this configuration, the load cells would experience the reaction forces on either side of the perch and the sum of their readings would represent the total weight of the perch and bird. Interestingly, wild adult birds have never been weighed accurately before so the accuracy threshold required for measurements to be useful is unknown. Upon Hickman's suggestion, an accuracy of 100g per bird was determined to be the objective. To better quantify this value, it was converted into a percentage of the average weight of a SGH (4kg), yielding an acceptable accuracy margin of 2.5%.

The next problem this design faced was the choice of sensing range, which was influenced by various factors. First, the wood forming the perch constituted a considerable amount of weight, approximately 3kgs. Using springs to counter the weight of the perch was considered, as a way of increasing weighing capacity. However, this simplification added complexity to the measurement process as all measurements would need to account for the displacement of the spring and factor this into their readings. Additionally the springs would introduce sources of uncertainty, further reducing the accuracy of the measurements. Finally, SGHs are destructive and would likely damage the springs. This approach was also rejected, as it was believed to pose more problems than it solved.

Large male SGHs can reach weights of up to 6 kg, but Hickman reported that it is rare for more than two birds to perch at the same time. Therefore, the scale's nominal load capacity was estimated at 15 kg, including the combined weight of two birds and a perch of approximately 3 kg. Standard load cells come in full-scale ranges of 1, 5, 10, 20 and 50 kg. While there would be more weighing capacity with two 20kg sensors, load cells specify temperature drift and non-linearity as a percentage of their full-scale (FS) measurement. Thus a trade-off between maximum allowable load and measurement accuracy had to be made. This informed the decision to choose two 10kg load cells, satisfying the load requirements of the system while retaining maximal accuracy. To prevent damage to the scales, consideration was given to a safety factor. The maximum overload of the available load cells was specified at 120% FS, giving a maximum safe load-bearing capacity of 24kg. Accounting for the nominal load of 15 kg, this gave a safety factor of 1.6 and allowed for another large male to perch safely on the scale.

Next the environmental exposure of the load cells was considered. The Kruger region is dusty and experiences a wide temperature range and occasional heavy rainfall. Since the load cells will be mounted outside the enclosure, it was determined that the load cells should have an IP65 weather rating. This informed the final choice of sensor: the TAL220 10kg load cell. Two of these load cells were ordered through Make Electronics, the only South African company which had online availability of these components.

Load cells typically consist of four strain-gauges in a full-bridge configuration as shown in [3.1.\[25\]](#)

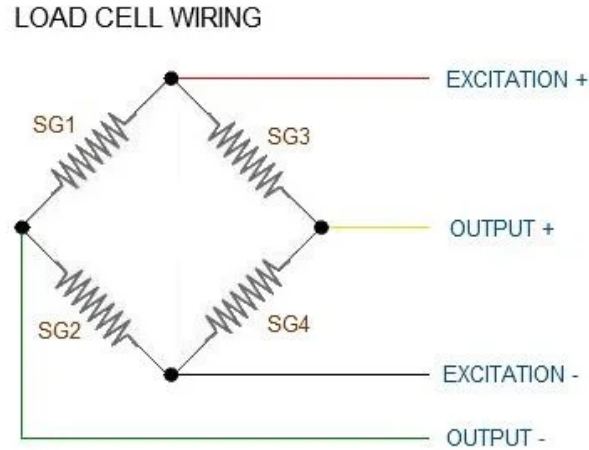


Figure 3.1: Wiring Diagram For Single Load Cell Testing

In environments with low voltage and low current, such as this project, the change in output voltage for a given change in loading stress is low and amplification is required to obtain measurements with higher resolution. The Hx711 amplifier module was chosen to interface with the load cells, both to minimise the complexity of designing separate amplification circuitry and because there are built-in arduino libraries for interfacing with this module. Additionally the Hx711 has a built-in 24 bit ADC, providing higher resolution than the arduino's built-in 12 bit ADC. The Hx711 also makes use of a 2-wire interface, reducing the wiring complexity and simplifying the construction process and future system maintenance.

TAL220s have an operable temperature range of -10°C to 55°C with a compensated temperature range of 0 to 40°C . Research has shown that while temperatures in the Kruger typically lie within the compensated temperature range of these sensors, they occasionally rise above 40°C . Since measurements taken at these temperatures would have unquantified temperature drift, it was determined that a temperature sensor should be incorporated into the design to quantify and correct measurement distortions. However, due to late arrival of the load cells, it was not possible to conduct the necessary tests to generate a lookup table and correction curve. Consequently, the design was modified to incorporate a confidence interval based on the ambient temperature when measurements occur. In the context of climate change and habitat destruction, temperature is a key metric in these birds' behavioural and physical data. The addition of the temperature sensor to account for inaccuracy in weight measurements had the added benefit of enriching the data set with temperature readings. The DS18B20 digital temperature sensor was chosen as it met all of the temperature sensor requirements as shown in the table below.

No.	Requirement	DS18B20
FS-6	5V operating voltage	3-5.5V operating voltage
FS-7	$<1\text{mW}$ standby power	$<1\text{mW}$ standby power
FS-8	9 bit resolution or better	12 bit ADC
FS-9	Operable temperature range $0-50^{\circ}\text{C}$	Operable temperature range $-55-125^{\circ}\text{C}$
FS-10	$\pm 0.5^{\circ}\text{C}$ accuracy or better over $0-50^{\circ}\text{C}$ temperature range	$\pm 0.5^{\circ}\text{C}$ accuracy over $-10 - 80^{\circ}\text{C}$ temperature range

Table 3.4: Functional specifications vs. DS18B20 Specifications

Additionally the DS18B20 is affordable (R40.18 from Mantech electronics) and has a well established arduino library.[\[26\]](#)

Initially the design included a speaker system to play the territorial cries of the SGHs, a strategy that has successfully attracted birds in previous research. However, Hickman cautioned against this approach as it might disturb the birds' natural behaviour and compromise the integrity of the data collected. Hickman pointed out that the SGHs always return to their nests, so additional measures to attract them are not required. As a result, this component was discarded.

In the early stages of the project design, the primary focus was minimising costs, as the initial designs relied on expensive power components which comprised a significant portion of the available budget. In light of this, Browning Trail camera traps, already owned by the APNR project, were incorporated into the design. To control the camera trap's Infra Red (IR) trigger, an IR LED connected to one of the arduino's GPIO pins was to be placed in front of it. Subsequently it emerged that there would not be exclusive access to these traps. At this stage, the design of the power circuitry had changed significantly, freeing a large portion of the budget. Consequently, using a separate camera to capture the image data was now feasible, which removed the complexity of disaggregating the shared camera data.

Selecting a suitable camera was the next design consideration. According to the literature, the birds' distinguishing feature for identification is their red throats. Therefore, the camera needed sufficient resolution to capture and identify this feature, and should perform well in low-light conditions. After evaluating various options, the ESP-32 CAM module which utilizes an OV2640 camera was chosen. This camera met the requirements as it satisfied all functional specifications(FS-1 to FS-5), it was affordable, stocked by the UCT white lab, and demonstrated good low-light performance. Hickman confirmed that it had the necessary resolution for the task.

3.4 Prototype design

The final prototype design consists of two 10 kg TAL220 load cells connected to an arduino mega via two hx711 amplification modules, a DS18B20 temperature sensor and an ESP-32 CAM with an OV2640 camera module as shown in [3.2](#).

3.5 Acceptance Test Procedures (ATPs)

3.5.1 Individual Load Cell Testing

To test the load cells, they were connected to an arduino via an Hx711 amplification module seen in [3.3\(a\)](#) and [3.3\(b\)](#) . The arduino mega was then used along with the hx711 arduino library [\[27\]](#) to read values from the load cells. For the single load cell ATPs, one side of each load cell was clamped to a table, with weights applied via a cable connected to the other side of the load cell. Four 2.5kg and two 5kg exercise weights were measured on a kitchen scale to confirm their masses and subsequently used as known weights for the acceptance test procedures.

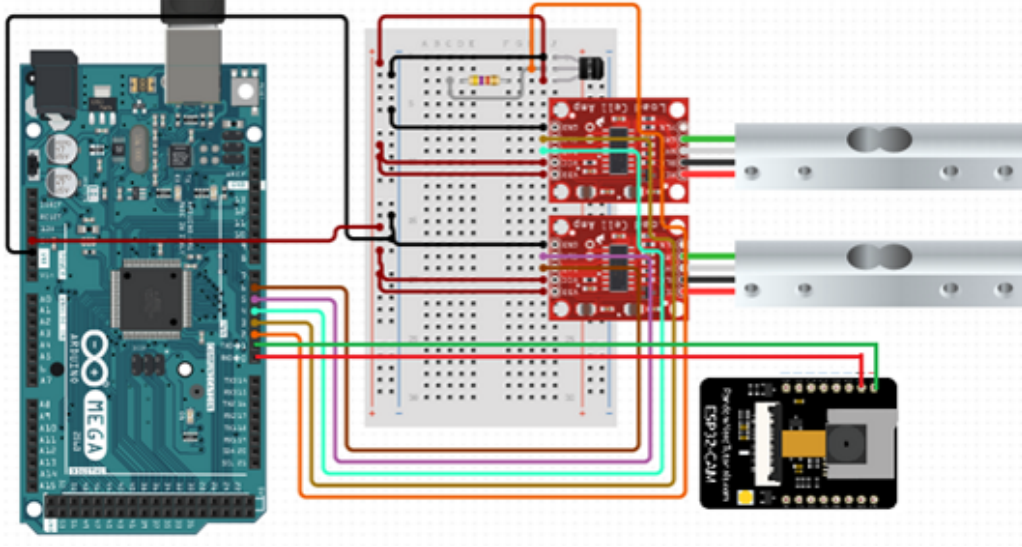
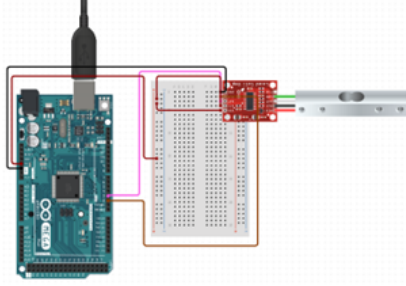
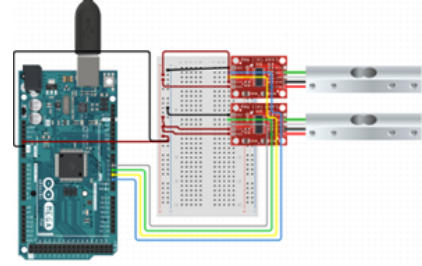


Figure 3.2: Wiring Diagram of final prototype



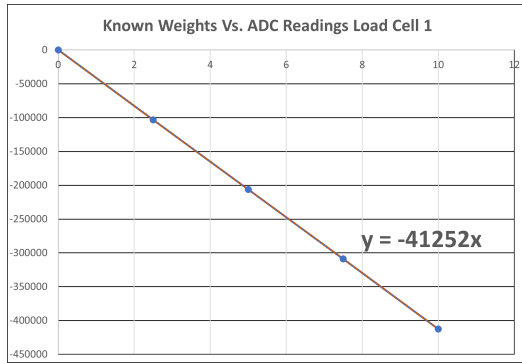
((a)) Single Load Cell



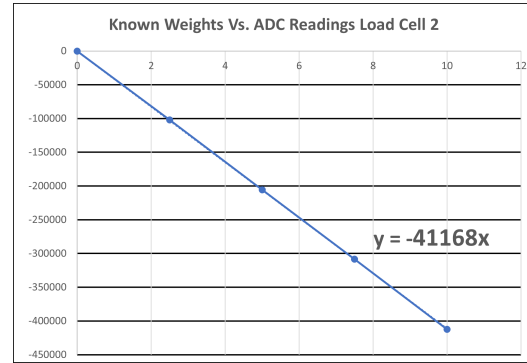
((b)) Double Load Cell

Figure 3.3: Wiring Diagrams

To determine the calibration factor of each load cell, the ADC of the hx711 was read without any weight on the scale, using the `scale.read()` function of the hx711 library.[27] which represents the zero offset. Known weights of 2.5, 5, 7.5 and 10 kg were then placed on the scale and the ADC digital values were measured and recorded. The zero reading was then subtracted from each value and the results were plotted against the known values. From this a regression line was fitted to the values (see graphs below) and was used to determine the calibration/ratio factor which converts ADC values to kilogram readings. All tests were run on a day when the ambient temperature was 21°C. The calibration factors of -41252 and -41168 for load cell 1 and 2 respectively were used for all subsequent testing.



((a)) ADC Values Vs. Known Weights Load Cell 1
With Slope of Regression Line



((b)) ADC Values Vs. Known Weights Load Cell 2
With Slope of Regression Line

Figure 3.4: Calibration Factors For Load Cell 1 and 2

The following tests were devised to evaluate the sensor's performance.

Zero Calibration Test

Description

Poll the load cell without any load placed on it. Record the measured value and subtract this from subsequent readings. Poll the load cell again with the zero reading subtracted. This reading should be less than 1 gram.

Result

Load cell 1- 10 separate measurements were taken as above, with the average calculated as 0.00032 kg. This is a 0.32 g error and passes the test.

Load cell 2- 10 separate measurements were taken as above, with the average calculated as 0.00046 kg. This is a 0.46 g error and passes the test.

Full-Scale Calibration Test

Description

After taring the load cell, place a 10kg mass on it. Read the output of the sensor and verify that the sensor reads the known weight with acceptable accuracy of 2.5%.

Result

Load Cell 1- 10 separate measurements were taken with the zero offset subtracted, yielding an average value of 9.8057 kg. This is an error of 1.94% and passes the test.

Load Cell 2- 10 separate measurements were taken with the zero offset subtracted, yielding an average value of 9.8177 kg. This is an error of 1.823% and passes the test.

Non Linearity Test

Description

Place a 2.5 kg weight on the load cell and record the measurement. Add another 2.5 kg weight and

record the measured value. Repeat this step until there is a 10kg weight on the load cell. Plot a graph of the known weights versus the measured weights and include a regression line. Calculate the maximum deviation of the actual graph from the regression line. Verify that the linearity error is within the TAL220's specified non-linearity error of $\pm 0.05\%FS$.

Result

This test was run with the averaged values of 10 readings at each known weight. It was determined that load cell 1 exhibited a maximum non-linearity of 0.047% FS while load-cell 2 exhibited a maximum non-linearity of 0.048% FS as seen in 3.6. Both sensors pass the test.

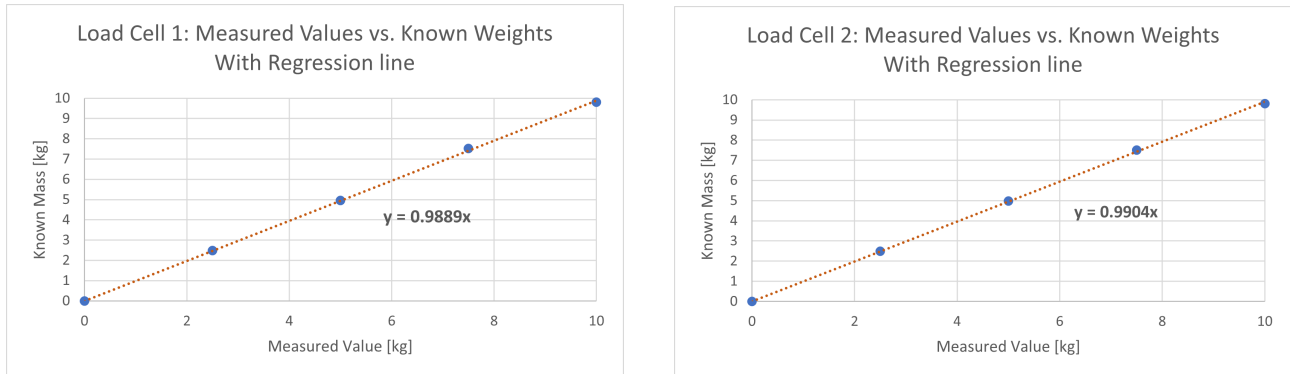


Figure 3.5: Measured Values vs. Known Weights With Regression Line For Load Cell 1 and 2

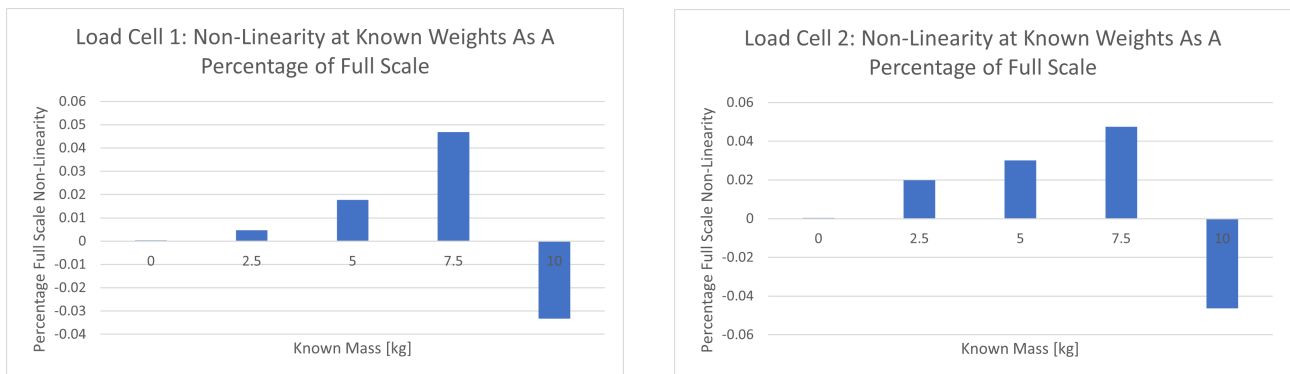


Figure 3.6: Non-Linearity at Known Weights As A Percentage of Full Scale For Load Cell 1 and 2

Repeatability Test

Description

Place a known weight on the load cell multiple times and record the measured weight each time. Calculate the repeatability error by comparing the measurements and finding a standard deviation. Verify that the standard deviation is less than 0.5% FS as specified on the TAL220 datasheet.

Result

Load cell 1 displayed a maximum standard deviation of 0.0064% FS while load cell 2 displayed a maximum standard deviation of 0.062% FS. as seen in 3.7. Both sensors pass the test.

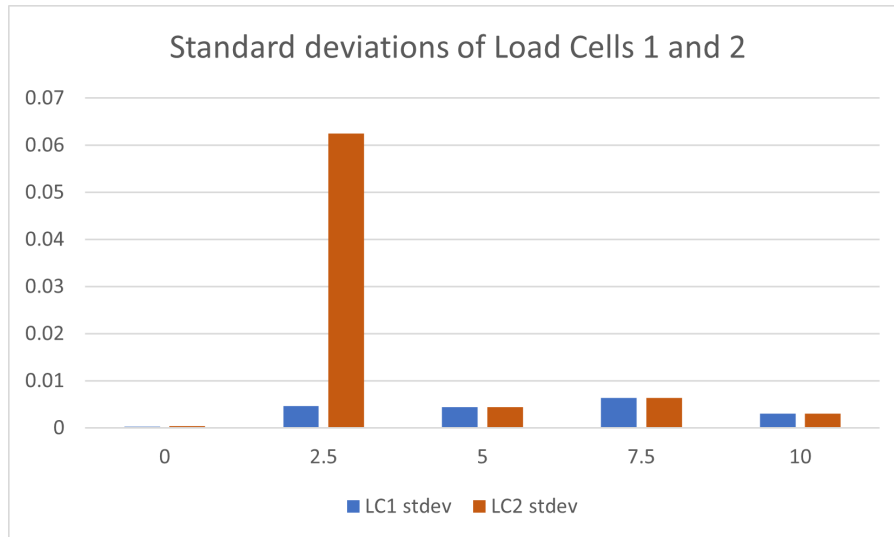


Figure 3.7: Standard Deviations of Load Cell 1 & 2

The results of the 10 tests run at each known weight are shown in 3.5

no.	0 kg	2.5 kg	5 kg	7.5 kg	10 kg
1	0.0002	2.4758	4.9646	7.522	9.8029
2	0	2.4763	4.9634	7.517	9.8094
2	0.0001	2.4811	4.96	7.5067	9.8022
3	0.0002	2.4765	4.9607	7.5092	9.8051
4	0.0004	2.4721	4.9597	7.5084	9.8027
5	0.0003	2.467	4.9627	7.5154	9.8071
6	0.0012	2.4821	4.9534	7.5234	9.8093
7	0.0005	2.4758	4.9632	7.5101	9.8045
8	0.0003	2.4772	4.9712	7.5065	9.8024
9	0.0001	2.4795	4.9652	7.5094	9.8101
10	0.0002	2.4831	4.9597	7.536	9.8165

((a)) Load Cell 1 Testing

no.	0 kg	2.5 kg	5 kg	7.5 kg	10 kg
1	0.0012	2.4788	4.9627	7.5067	9.8094
2	0	2.4763	4.9534	7.5092	9.8022
2	0.0002	2.4851	4.9632	7.5084	9.8051
3	0.0004	2.4745	4.9712	7.5154	9.8027
4	0.0001	2.4821	4.9652	7.522	9.8071
5	0.0002	2.4673	4.9597	7.517	9.8093
6	0.0012	2.4901	4.9646	7.5234	9.8045
7	0.0007	2.4758	4.9634	7.5101	9.8024
8	0.0003	2.4662	4.96	7.5065	9.8029
9	0.0005	2.4765	4.9607	7.5094	9.8101
10	0.0003	2.6831	4.9597	7.521	9.8075

((b)) Load Cell 2 Testing

Table 3.5: Load Cell 1 & 2 Testing

3.5.2 Combined Load Cell Testing

The combined load sensor testing was carried out by attaching a load cell to either end of a dowel stick. The other end of each load sensor was bolted to a flat wooden block. Known masses were placed on the dowel and readings from both load cells were summed to determine the total weight on the scale.

Combined Full Scale Calibration Test

Description

Place a known weight that is the sum of the maximum expected weights on both sensors combined (20

kg). Read the outputs and verify that the combined weight is read with an acceptable accuracy of 2.5%

Result

10 separate measurements were taken with the zero offset subtracted, with an average value of 19.7641 kg. This is an error of 1.18% and passes the test.

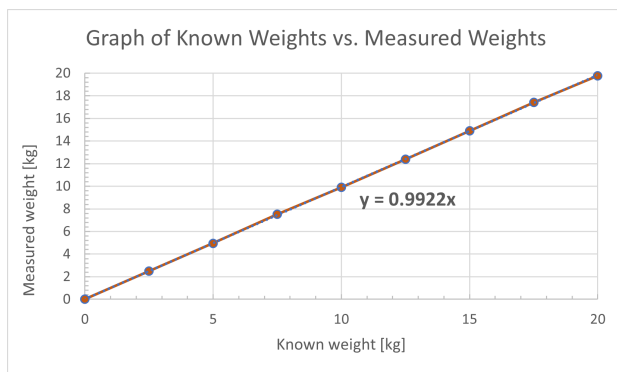
Combined Linearity Test

Description

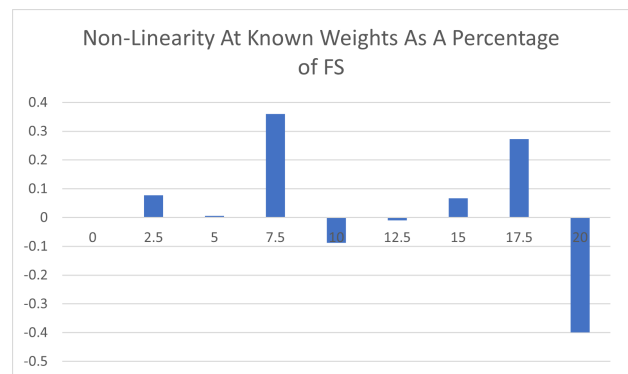
Place a 2.5 kg weight on the load cell and record the measurement. Add another 2.5 kg weight and record the measured value. Repeat this step until there is a 20kg weight on the scale. Plot a graph of the known weights along with a graph of the measured weights and include a regression line. calculate the maximum deviation of the actual graph from the regression line. Verify that the linearity error is within the TAL220's specified non-linearity error of $\pm 0.05\%FS$.

Result

This test was run with the averaged values of 10 readings at each known weight. [3.8\(a\)](#) It was determined that the scale exhibited a maximum non-linearity of 0.41% FS [3.8\(b\)](#) this passes the test.



((a)) Graph Of Known Weights vs. Measured Weights With Both Load Cells



((b)) Non- Linearity Error With Both Load Cells

Combined Repeatability Test

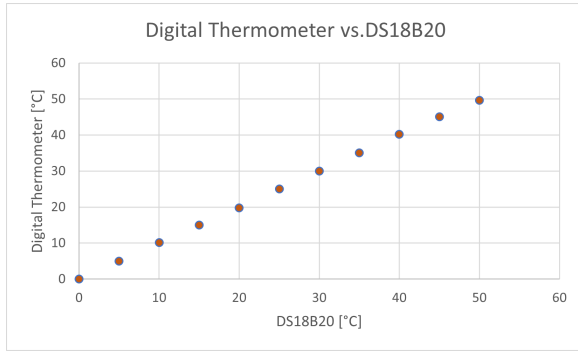
Description

Place a known weight on the scale multiple times and record the measured weight each time. Calculate the repeatability error by comparing the measurements and finding a standard deviation. Verify that the standard deviation is less than 0.5% FS as specified on the TAL220 datasheet.

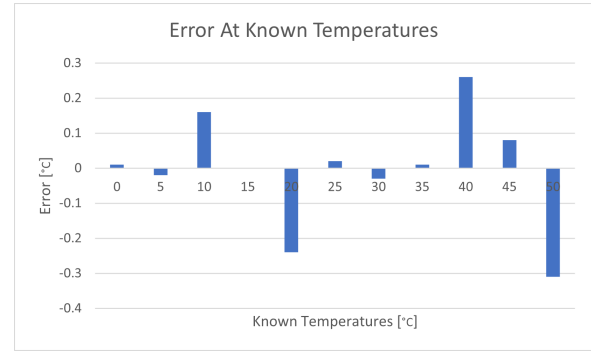
Result

The combined scale displayed a maximum standard deviation of 0.456% FS as seen in [3.9](#). The combined scale passes the test.

3.5. Acceptance Test Procedures (ATPs)



((a)) Digital Thermometer vs. DS18B20



((b)) Error at Known Temperatures

Figure 3.10: DS18B20 Input Ouput Curve and Error Hisogram

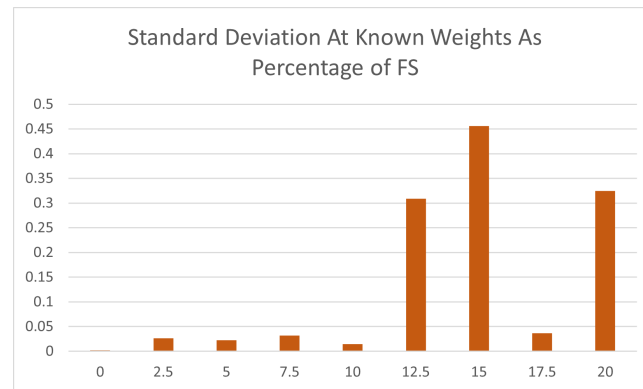


Figure 3.9: Standard Deviation Of Combined Load Cell Set Up

3.5.3 Temperature Sensor Testing

Accuracy Test

Description

Place the temperature sensor in a hot water bath. Use a digital thermometer to acquire reference values and sample the temperature at intervals of 5°C and compare the readings from the temperature sensor with the reference temperatures. Confirm that the maximum error does not exceed the 0.5°C maximum error specified in the DS18B20 datasheet.

Result

A temperature range of 0-50°C was examined in testing since this is representative of the maximum temperature variation experienced in the kruger. This is shown in 3.10(a). The DS18B20 was found to have a maximum error of 0.31°C as seen in 3.10(b). The sensor passes the test.

3.5.4 Camera Testing

Description

Set up the camera module in a well-lit room with natural daylight. Take a photo of an object with detailed red and black on it. Move the camera module to a dimly-lit room or area with low light and record another picture. Evaluate the performance of the camera.



((a)) Low-light Conditions



((b)) Bright-light Conditions

Figure 3.11: Test Photos

Result

In order to evaluate the quality of this test, sample photos [3.11](#) were sent to Hickman. The photos were confirmed to be acceptable and the camera passes the test.

3.6 Conclusion

Throughout the development process, careful design considerations were taken into account to ensure the optimal performance of the system. The acceptance test procedures designed to evaluate the sensing circuitry's performance were conducted. All acceptance test procedures yielded positive results demonstrating the success of the sensing system. Overall, the successful implementation of the sensing circuitry has significantly advanced researchers' ability to monitor and study SGHs in their natural habitat, contributing to the ongoing conservation efforts. Data acquired with this system will further enhance knowledge of these birds' health and behavioral patterns, supporting targeted conservation strategies and fostering a deeper understanding of their ecological needs.

Chapter 4

Processing Hardware and Device Enclosure

4.1 Introduction

At its foundations, the objective of this project is to optimise the manner in which members of the Fitzpatrick Institute of African Ornithology record data regarding SGHs within APNR deployment sites in the Kruger. The implementation of autonomous sensing, as a means of optimisation, relies heavily on the use of a microcontroller to facilitate the capture of data by the peripheral sensor circuitry and perform data processing. In addition to this, for the system to be feasibly deployable in the field, the microcontroller and peripheral circuitry require an enclosure that protects the circuitry from environmental conditions within the Kruger.

This section provides an overview of both the processing hardware and the hardware enclosure, including the design choices made in the implementation of these two systems alongside the acceptance test procedures (ATPs) that were utilised in evaluating either systems' performance. The section concludes with an analysis of the results of these ATPs.

4.1.1 Functional and Technical Requirements

The design process was guided, at its genesis, by the functional requirements supplied by the stakeholder's problem statement. The following requirements provide a baseline for the expected functionality of the processing hardware and enclosure:

- FR-1: The system must be light and portable such that it can be easily mounted at the nest sites.
- FR-2: The system's hardware must be protected by a robust enclosure.
- FR-3: The system must be able to tolerate temperatures from 0-45°C.
- FR-4: The system must trigger all data capture processes when a threshold value is registered.
- FR-5: The system's battery life must last for 2 weeks without stakeholder intervention.
- FR-6: The system enclosure must conform to small dimensions as to be easily hidden from the SGHs.
- FR-7: The system enclosure must not break if loaded in static and/or dynamic compression.
- FR-8: Data must be stored on an SD card that can be removed from the device without removing the device from the nest site.
- FR-9: The system must conform to a budget of R2000.
- FR-10: The system must be able to tolerate heavy seasonal rainfall and dust conditions present in the Kruger.

The technical requirements outlined below in Table 4.1 and Table 4.2 build on the functional requirements above.

Table 4.1: Table outlining technical requirements for microcontroller

Label	Requirement
TR-1	5V operating voltage
TR-2	Supplies regulated 5V to peripherals
TR-3	Operating temperature between 0-45°C
TR-4	Must have sleep modes
TR-5	7KB of dynamic storage space
TR-6	At least 15 Digital I/O pins
TR-7	Active current draw less than 200 mA from batteries
TR-8	Easily implementable coding interface
TR-9	Low idling current draw
TR-10	24 bit ADC

Table 4.2: Table outlining technical requirements of hardware enclosure

Label	Requirement
TR-11	IP64 Rated
TR-12	Tolerates temperatures of 45°C without deformation
TR-13	Conforms to dimensions of 15x15x10 cm
TR-14	Withstands compressive load of 20kg
TR-15	Passive heat dissipation
TR-16	IK04 resistant to concentrated impact

4.2 Theory

4.2.1 Enclosure Ratings

The International Electrotechnical Commission (IEC) standard provides a system for rating the varying degrees of protection provided by enclosures of electrical equipment [28]. This system ranks enclosures according to their Ingress Protection (IP) rating. The IP rating is determined by the enclosure itself, alongside the manner in which the enclosure is fixed. This refers to the lid sealing, cable entry points and material durability [29].

The IP rating is a two-digit grading system applied to the enclosure of both mechanical and electrical systems which gives insight into the ability of the enclosure to protect against various types of intrusion into the enclosure [30]. The forms of resistance to intrusion can be subdivided into three groups: the intrusion of the user into the enclosure, the intrusion of foreign bodies such as dust, dirt and other solid matter and the intrusion of water/moisture. The standard for the depiction of IP ratings consists of the letters ‘IP’ followed by two digits. The first digit is a number between 0 and 6, indicating the degree of protection from the ingress of solids [30]. A rating of 0 specifies that no protection is afforded, lower ratings of 1 and 2 pertain to resistance to the hand and the finger coming into contact with the inside of the enclosure whilst higher ratings indicate protection against probes of around 1mm (based

on rating) and protection against dust. The second digit spans 0 to 9 and indicates the resistance to ingress of moisture at varying pressures, exposure types (immersion/drip), angles and depths based on how high the rating is. These digits may be followed by supplementary letters which indicate resistance to certain specified hazards. Table 4.3 depicts the IP ratings and their associated levels of protection [29].

Rating (Solids)	Ingress Protection Requirement	Rating (Moisture)	Ingress Protection Requirement
0	No protection	0	No protection
1	50 mm diameter sphere	1	Vertical water drops
2	12.5 mm diameter sphere	2	Vertical water drops at 15° tilt
3	2.5 mm diameter probe	3	Water spray at 60° from vertical
4	1 mm diameter probe	4	Water splash from all directions
5	Majority dust (no harmful deposit)	5	Low pressure jets from all directions
6	All dust	6	High pressure jets of water from all directions
NA	NA	7	Immersion between 15 cm and 1 m
NA	NA	8	Longer immersion periods at higher pressure
NA	NA	9K	High pressure/temperature jet sprays

Table 4.3: Table IP ratings for resistance to ingress of solid matter and moisture

Examples of supplementary letters include H (High voltage), M (Tested in motion), S (Tested at rest), W (Specified Weather conditions). Additional metrics of enclosure functionality include the IK rating [31]. In a similar manner to IP ratings, IK ratings are defined as ‘IK’ followed by a number from 0 to 10. This number depicts the degree of protection provided by the electrical enclosure against external mechanical impacts. IK ratings are verified through the use of a Charpy Testing machine. An enclosure IK rating listed as IK04 indicates that the enclosure is protected against 0.5 J of impact which is the equivalent impact of a 0.25 kg mass dropped from 200 mm above the impacted surface [31].

4.3 Design Choices

The choice of microcontroller was governed by requirements laid out by the power and sensing circuitry alongside the software submodule. For the full autonomous scale system to function, the microcontroller needed to fulfill the requirements placed on it by each submodule. These requirements are further discussed below:

The initial requirement considered in guiding this design decision was the ease of interfacing between the peripheral sensor circuitry and the microcontroller. In the early stages of the design, the sensor circuitry comprised solely of two TAL220 10kg load cells, two HX711 voltage amplifiers and a Browning Trail camera trap that was already owned by the APNR project. The Browning Trail camera was to be triggered via its IR trigger using an IR LED connected to a GPIO pin of the microcontroller. Thus, the Browning Trail camera trap did not contribute much complexity in the way of software implementation. Interfacing with the HX711 modules and load cells, however, was a more complex task. It was decided that, in an attempt to simplify the coding process, an Arduino Mega 2560 microcontroller would be the first architecture considered for use. This is due to the extensive built-in Arduino libraries available for interfacing with these voltage amplifiers alongside numerous other sensor modules. It was further foreseen that should any other sensors need to be implemented at later stages of the design, the built-in Arduino libraries would streamline this task. In addition to the requirements placed on the ease of software interfacing, the microcontroller needed to be capable of delivering sufficient output voltage

and current to the sensing circuitry. The load cells required a 5 V supply to operate and the HX711 operated off of 2.6-5.5 V. It was verified that an Arduino Mega 2560 can source a regulated 5 V from an internal LM358LIST voltage regulator and its digital pins can source a maximum of 40 mA which far exceeds the 1.5 mA requirements of the HX711. Whilst the Arduino Mega 2560's 12 bit on-board ADC fell short of the technical requirements, the HX711's built-in 24 bit ADC catered for this shortcoming on the part of the Arduino. Consequently, the Arduino Mega 2560 remained a viable option at this point of the design.

It was later learned that this project would not be provided with continuous access to the Browning Trail camera during deployment. Consequently, the microcontroller would need to interface with a separate camera. The ESP-32 CAM module was chosen due to it being readily accessible in the lab and being cost effective. The camera module utilizes an OV2640 camera which, while not as functional as the Browning trail camera, was verified to be suitable for the scenario by the stakeholders. An issue arose, however, in the increased power draw present as a result of the ESP-32 CAM. The nature of the Arduino Mega 2560 having multiple sleep modes became imperative in reducing the power drawn from the batteries. Moreover, the addition of a DS18B20 temperature sensor for the purpose of quantifying load cell temperature drift at temperatures in excess of 40°C further cemented the practicality of the extensive Arduino libraries available for sensor interfacing.

3.4 Power Tree

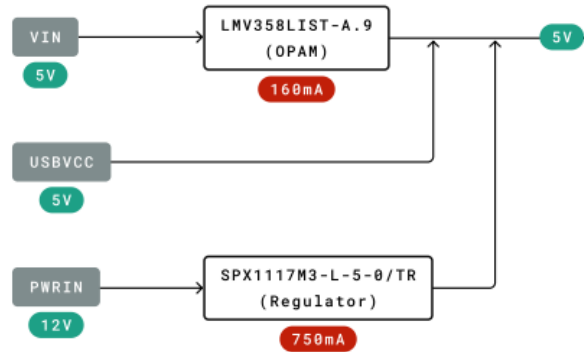


Figure 4.1: Figure depicting Arduino Mega 2560 Power tree

The next requirement that needed to be met was the limitation placed on the amount of power drawn by the microcontroller. In the early stages of the project, it was found during power budgeting that, in order to meet the required 2 week system lifespan, the microcontroller could not exceed a maximum current draw of 200 mA. As depicted in Figure 4.1 referenced from the Arduino Mega 2560 datasheet, the Arduino Mega 2560's internal LM358LIST has a maximum active current draw of 160 mA which falls within the required limit. The power submodule provides the microcontroller with 5 V from an LM317T voltage regulator circuit resulting in a maximum power dissipation of 800 mW sourced from the power submodule. For the sake of benchmarking, this was compared to the Raspberry Pi Zero W V1.1 which was readily available in the labs at a similar price to the Arduino. The Raspberry Pi Zero W V1.1, supplied with 5.19 V, draws 120 mA whilst idling yielding a maximum power dissipation of 622.8 mW [32]. The Raspberry Pi Zero W V1.1 does not, however, have any sleep modes and therefore

draws this power continuously. Consequently, the Arduino Mega 2560's power dissipation was found to be preferable. It was further noted that the Arduino Mega 2560 had 6 different sleep modes that could be used to minimise current draw.

Following this, it came under consideration as to whether the Arduino Mega 2560 had enough Dynamic and Flash memory to store the code written for the various processes that the automatic scale conducts. Test scripts were written for the purpose of benchmarking the amount of Flash Memory and RAM that the program and associated variables (local and global) would need. The estimated usage suggested that the memory requirements that the microcontroller needed to fulfill was 6KB. Consequently, the technical requirements were set at 7KB to provide some headroom. It was determined that the Arduino Mega 2560 has 4KB of EEPROM (for program storage) and 8KB of internal SRAM (for storage of variables) thus surpassing the requirements for program and variable storage. During software benchmarking, it was noted that the Arduino Mega 2560 did not have an on-board SD Card slot and therefore could not write the received sensor measurements to an SD card. This was a hard functional requirement, however, and so a Micro-SD breakout board was sourced for the Arduino.

After verifying that the Arduino Mega 2560 met all the technical requirements as depicted in 4.4, the Arduino Mega 2560 was confirmed as the microcontroller to be used and ordered from Make Electronics at a cost of R319.00.

Label	Requirement	Specification
T1	5 V operating voltage	Operating voltage of 5-12 V
T2	Supplies regulated 5 V to peripherals	Has a regulated 5 V output pin
T3	Operating temperature between 0-50°C	Can operate between -45-80°C
T4	Must have sleep modes	6 sleep modes
T5	7 KB of dynamic storage space	8 KB of dynamic storage space
T6	At least 15 Digital I/O pins	54 Digital I/O pins
T7	Active Current draw less than 200 mA from batteries	Maximum current draw of 160 mA
T8	Easily implementable coding interface	Extensive Arduino libraries
T9	Low idling current	20 mA consumption in sleep mode
T10	24 bit ADC	24 Bit ADC interfaced by HX711

Table 4.4: Table comparing technical requirements to Arduino Mega 2560 specifications

The design choices made regarding the enclosure were guided by the demands of the landscape wherein deployment would occur, alongside the temperament of the SGHs. The APNR SGH project is located on the western boundary of the Kruger National Park [33]. The Kruger is a dusty region that experiences a wide range of temperature and rainfall conditions. In addition to this, the stakeholders advised that SGHs are extremely aggressive birds and tend to destroy any hardware that is exposed to them. Consequently, the enclosure design needed to ensure sufficient protection of internal circuitry from the environment whilst being durable and sufficiently small to be hidden from the SGHs.

To mitigate temperature stress on the internal circuitry, the functional operating temperatures of the hardware needed to be addressed. Research illustrated that the average maximum temperature within the Kruger lies between 30°C and 35°C with occasional spikes above 40°C [34]. The Arduino Mega 2560 and peripheral sensor circuitry can operate in a temperature range of -40°C to 85°C and therefore pose no issues regarding the temperature extremes within the Kruger. These components merely served

to guide the dimensions of the enclosure. A vital consideration to the health of the system, however, was the potential for the Lithium-Ion batteries to enter thermal runaway given the extended exposure to temperatures in excess of 30°C. Consequently, this informed the decision that the enclosure must be able to handle maximum temperature conditions of 45°C without damage to itself or the components within. In addition to this, precipitation in the region reaches an average seasonal high of 94 mm over the highest rainfall months of the year. Moreover, maximum average wind speeds reach 23.6 km/h. As a result of these conditions, it was decided that the enclosure would need to meet the IP64 rating.

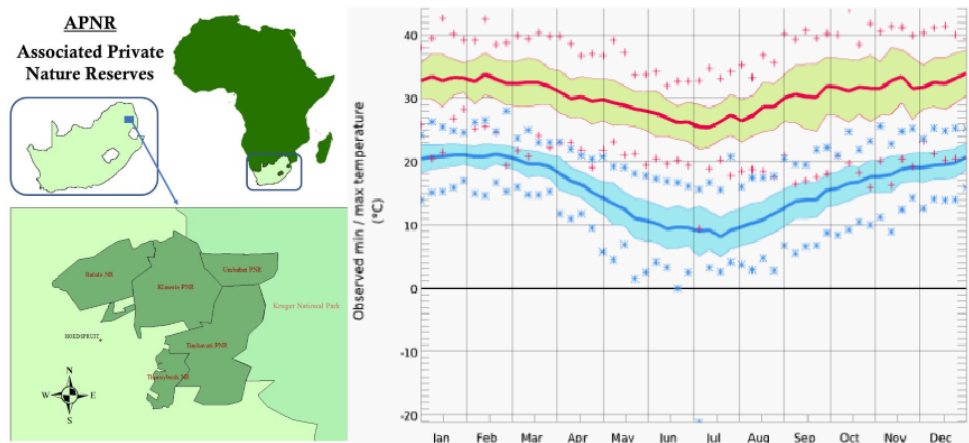


Figure 4.2: Figure depicting deployment sites in the Kruger and maximum temperature ratings over 30 years

Guided by the IP64 rating, the material type used for the enclosure needed to be determined. In the early stages of the design project, budgetary constraints were a concern as the initial design of the power submodule relied on expensive components that took up a significant portion of the budget. This resulted in the initial decision that the enclosure be made out of plastic. This would allow for the enclosure to be 3D printed with ease which would be both functional given the ease of regular prototyping that a 3D printer offers and cost effective due to there being ready access to a 3D printer. Notably, 3D printed parts would not be sufficient in forming a near hermetic seal at any join points given the tolerances involved with 3D printing. Thus, the following design decisions arose as solutions to the shortcomings of 3D printed parts.

In order to attain a proper seal from moisture and dust, it was decided that a gasket would be implemented at the join between the enclosure base and lid. In addition to this, the Arduino Mega 2560 and HX711 modules required cable connections to sensing circuitry outside of the enclosure. Thus, cable entry points to the enclosure would require cable glands in order to ensure a proper seal. The initial choice of using plastic for the lid was reconsidered upon realisation that the enclosure had no way of dissipating any of the heat building up internally. No venting points could be added to the enclosure design as this would compromise the enclosure's resistance to the ingress of dust and moisture. Consequently, a second iteration of the enclosure was designed which consisted of a plastic enclosure base, sealed with a gasket and cable glands for the electronics, however the lid was to be made out of metal and designed to act as a heatsink to dissipate internal heat. While this would not actively cool the internal electronics, the heatsink ensures that dissipation of internal heat occurs. The introduction of this heatsink was guided by the need to minimise the possibility of thermal runaway

in the batteries. Notably, late arrival of parts raised concerns as to whether parts would have to be re-ordered through another supplier and therefore what remained of the budget needed to be conserved. This led to the second iteration of the enclosure design being abandoned due to the monetary costs of sourcing a suitable heatsink and the time required to do so.

The use of a 3D printer raised queries into the type of plastic to be used for the enclosure and the relative viability of the plastic given the environmental heat and UV exposure. Two plastic types were considered for the enclosure, with the selection of these types being limited by the capabilities of the 3D printer that was available. These two plastic types were Polylactic Acid (PLA) and Polyethylene Terephthalate-glycol (PETG). Research on the material characteristics of PLA and PETG was conducted to inform the decision regarding plastic types. It was found in a study analysing the effect of accelerated aging on PLA and PETG through prolonged (24h) UV-C exposure that this exposure reduced the overall mechanical properties of PLA by 6-8% whilst the mechanical properties of PETG were reduced by over 30% [35]. This was represented by a 9.1% loss in tensile strength for PLA and a 38.1% loss in tensile strength for PETG. PLA samples depicted a compressive strength loss of 13.1% and, contrasting this, there was a 33.9% loss in compressive strength for PETG. Furthermore, the glass transition temperatures of PLA and PETG were found to be 60-65°C and 80-82°C alike [36]. Whilst the glass transition temperature of PETG is higher than PLA, PLA is suitable for environment temperatures of 45°C. In light of these insights, white PLA was selected for use in prototyping the enclosure.

The enclosure was designed in Fusion360 to optimise dimensions and component placement for the specific hardware used and to allow for an STL file to be generated for printing. The placement of electronics within the enclosure needed to be strategically managed to ensure that all wiring could easily reach the Arduino without the need for excessive cable management. Additionally, the SD card needed to be easily accessible and, in the case of future iterations, the battery placement needed to be close to the heatsink. Notably, in order to ensure as few entry points for moisture and dust as possible, screw points passing from the inside of the enclosure to the outside were minimised by providing risers inside the enclosure to which screws could be fastened. This is depicted in Figure 4.3. Moreover, the introduction of an indent on the lip of the enclosure top allows for the placement of a gasket without significantly obstructing the ability of the lid to seal to the enclosure. The risers and lip are present on both the enclosure base and the enclosure cover as depicted in Figure 4.3.

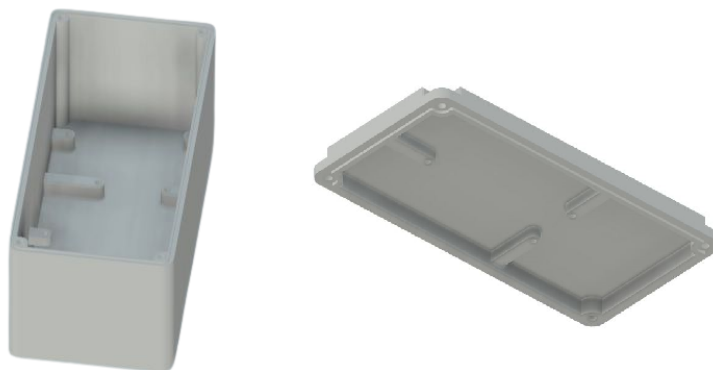


Figure 4.3: Figure depicting parts drawn in Fusion360

In addition to the main enclosure design, an enclosure needed to be made for the ESP-32 CAM that was deployed externally to the main device enclosure. The main enclosure was resized to fit the ESP-32 CAM and printed as a separate enclosure for the ESP-32 CAM.

4.4 Final Design

Once the parts had been printed, the dimensions of the parts were verified against the dimensions of the electronic hardware. The Arduino Mega 2560, LM317T voltage regulator and SD breakout module were fitted to the enclosure as depicted in Figure 4.4. Following this, a gasket was fitted to the lining of the enclosure and the battery housing and HX711 modules were fitted to the risers of the lid.

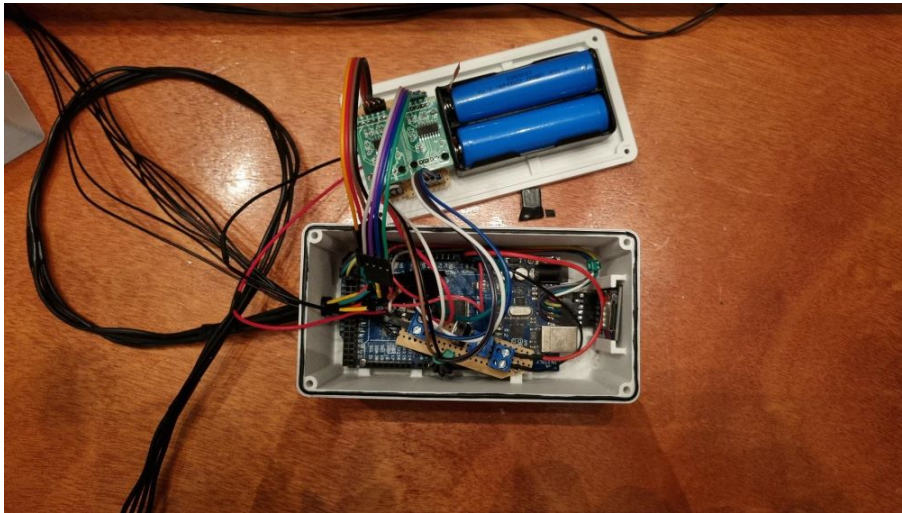


Figure 4.4: Figure depicting the enclosure base and lid with assembled hardware

A second fully assembled enclosure was printed and used for testing. This enclosure is depicted in Figure 4.5. Notably, the cable glands ordered did not arrive and could not be sourced otherwise. Hence, they were replaced with O-rings that could be sourced. These O-rings, whilst functional, would not form the necessary seal to meet IP64 ratings. Consequently, all final ATP testing was conducted on the enclosure without the hole for the passage of sensor wires.



Figure 4.5: Figure depicting the full assembly

4.5 Acceptance Test Procedures

ATP Label	Test Description	Test Result
ATP-1.1	Current draw is measured at input to Arduino Mega 2560 on start-up. Acceptance criteria: Current draw does not exceed 200 mA.	Active current draw at input was measured at $\pm 150\text{ mA}$.
ATP-1.2	Device is put into sleep mode and current draw is measured. Acceptance criteria: Current draw does not exceed 25 mA.	Current draw at input in sleep mode was $\pm 20\text{ mA}$
ATP-1.3	Code is uploaded to microcontroller. Acceptance criteria: Code does not exceed storage capacity.	Global variables required 9.2 KB resulting in the Arduino crashing as the size of dynamic memory is 8 KB.

Table 4.5: Table depicting Acceptance Test Procedures for microcontroller

ATP Label	Test Description	Test Result
ATP-2.1	Moisture ingress: The enclosure is sprayed by a spray nozzle from a maximum distance of 200 mm at a 180° angle from the vertical. The test duration is 5 minutes. Litmus paper is used as a visual indicator as to whether moisture infiltrated the enclosure. Acceptance criteria: No visual change in Litmus paper.	The spray nozzle used was a 17 mm diameter garden hose. After 5 minutes, the enclosure was opened and the Litmus paper visually inspected. The Litmus paper showed no obvious signs of being wet or colour change.
ATP-2.2	Solids ingress: The enclosure is placed in a sealed box with an entry point for placement of a leaf blower. Sand with small stones and soil is placed in the box along with the enclosure. The leaf blower is then turned on. Acceptance criteria: Visual inspection shows no ingress.	The test was conducted for a duration of 3 minutes. While the outside of the enclosure was mildly blemished, no solids were found inside the enclosure upon opening.
ATP-2.3	Temperature stress: The enclosure is placed in an oven and heated to 45°C for 20 minutes. Acceptance criteria: Enclosure does not show signs of softening or warping.	Physical inspection showed that the material remained hard and brittle.
ATP-2.4	Compressive stress: Enclosure is placed in an Instron UTM machine with a single point flexure test acting on the lid. Acceptance criteria: Enclosure does not fracture.	The test was limited to a load of 30 kg, however the enclosure showed no imminent signs of failure.
ATP-2.5	Impact stress: A 300 g hammer is dropped on the enclosure from height intervals increasing in gaps of 10cm to mimic SGH beak impacts. Acceptance criteria: Maximum force exerted by SGH unknown. Success determined by IK04 rating.	The enclosure fractured when impacted from a height of 1.8 m.

Table 4.6: Table depicting Acceptance Test Procedures for device enclosure

4.6 Discussion of Test Results

The results of ATP-1.1 indicated that the microcontroller did not have sufficient Dynamic storage to upload all of the code. The size of storage could not be altered at this point of the project, hence the code was reduced in size. This was done by shortening the lengths of the arrays used to store weight measurements during data recording. After shortening these arrays, the global variables fit within the Arduino's Dynamic memory.

Notably, the functionality of the Arduino Mega 2560 in providing sufficient voltage and current to the peripheral circuitry was verified when testing the overall automatic scale system. It was further verified that the Arduino successfully read measurements from the load cells and stored these measurements on the SD card present on the breakout board. Moreover, it was verified that the Arduino pulled the GPIO pin of the ESP-32 CAM high thus triggering a photograph during weight measurements. More intensive tests could not be conducted on the Arduino due to the sensing circuitry and software module requiring priority access to the Arduino in order to ensure the overall system functioned. The lack of organised access to the Arduino for testing arose as a result of very late arrival of the delivery from Make electronics.

The results of ATP-2.1 and ATP-2.2 indicate that the enclosure was successful in achieving an IP64 rating. The true resistance to ingress of dust, however, cannot be accurately determined in this manner. The requirement that must be met for a solids ingress rating of 4 is placement of the enclosure in a Dust chamber after which no ingress must be observed. The Materials lab at the University of Cape Town (UCT) was contacted to determine whether this test could be conducted, however, the hardware required was unavailable. Hence, the test was simulated outside of lab conditions as indicated.

ATP-2.3 depicts that the enclosure material was suitably chosen to be able to withstand extreme temperatures within the Kruger, thus meeting the technical requirement of tolerance between 0-45°C. After verifying that the enclosure withstood 45°C the test was extended to increase in intervals of 5°C every 10 minutes until a noticeable change occurred in the material quality. At 65°C it was found that the consistency of the PLA had changed to that of a hard rubber. This aligns with the expected glass transition temperature for PLA.

The Materials lab at UCT was contacted to conduct both quasi-static and dynamic load tests on the enclosure in an attempt to simulate interactions that SGHs may have with the enclosure. These tests aimed to simulate a SGH sitting on the enclosure as well as attacking the enclosure with its beak. A compressive loading test was successfully set up at the Materials lab using an Instron UTM machine as depicted in Figure 4.6.

The enclosure was loaded linearly from 0 N to 300 N at a rate of 1 mm per minute. As can be seen from the linear nature of Figure 4.7, the enclosure remains rigid up until 300N (30kg). Consequently, the enclosure passed the ATP. Notably, the enclosure was not tested to failure as, due to the time constraints of the project deadline and the net printing time for one enclosure being 18 hours, there was only sufficient time to print one prototype for testing.

A further request was put in at the Materials lab for the use of the Zwick Pendulum Charpy Impact test machine. The machine, however, required test samples to be of a specific shape and dimension.

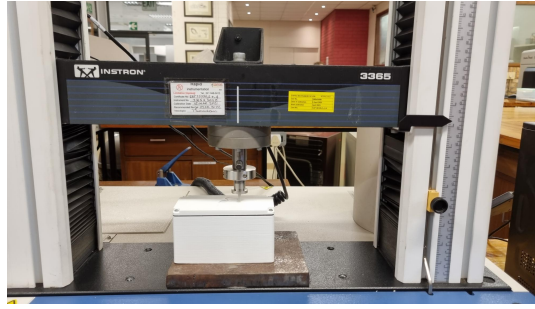


Figure 4.6: Figure depicting enclosure undergoing compressive loading test

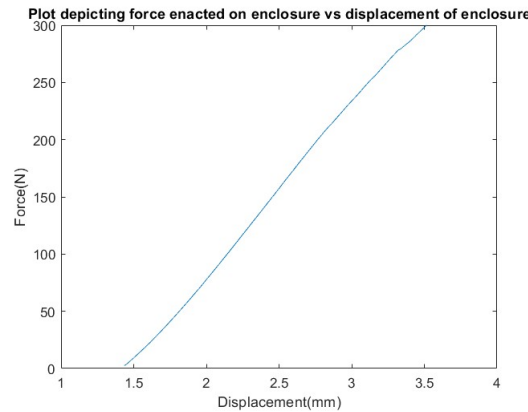


Figure 4.7: Figure depicting data gathered during compressive loading test

Due to limited time constraints this could not be printed. In an attempt to simulate this test, the stakeholders were contacted to find out the striking force of the SGH beak. The stakeholders did not know the striking force of the SGH, however, and this information could not be sourced online. Hence IK04 ratings were selected as a baseline for a measure of test success. Consequently, the impact test was run outside of lab conditions according to the test guidelines using a 0.3 kg hammer as provided by the IK ratings. It was found that the enclosure failed to meet IK04 standards. This test, however, was inaccurate given that the same sample was used for multiple impacts. Additionally, gross inaccuracies in the manner of measurements taken were present as the true impulse imparted on the material was unknown. It is recommended that this test be re-performed in the lab in following iterations.

4.7 Conclusion

The implementation of processing hardware as well as a hardware enclosure within the greater project scope was guided by requirements laid out by the power and sensing circuitry alongside the software submodule. The evolution of this section was propelled by numerous design choices, with the successes of these design choices evaluated using acceptance test procedures. The microcontroller successfully met the ATPs laid out for it after adjusting the code, whilst the device enclosure met all ATPs barring the impact test. Notably, certain tests conducted on the hardware enclosure would be better conducted within lab conditions as discussed in the results analysis. This is recommended for future iterations of enclosure prototype testing. The design and implementation undertaken in this section has provided a strong basis for future developments. Perhaps of most consequence, the implementation of this system has markedly improved the stakeholder's methods of data capture within their study of SGHs.

Chapter 5

Data Processing

5.1 Introduction

In the current landscape of interconnected systems, where devices and networks communicate seamlessly, the number of sensors and input devices has increased rapidly. These devices result in an exponential surge in data generation. This unprecedented influx of data presents both opportunities and challenges, allowing for the implementation of robust data processing techniques to extract meaningful insights and facilitate informed decision making.

This subsection provides an overview of the data processing methodology used to convert raw sensor data into valuable information. It includes data acquisition, pre-processing, filtering, and storage, resulting in accessible and user-friendly data for easier interpretation and analysis.

In the data processing pipeline, the first step is data acquisition. Sensors and input devices capture real-time data on Southern Ground Hornbill weights and surrounding temperature.

After data acquisition, pre-processing is essential to prepare the raw data for subsequent analysis. Tasks include cleaning and formatting to ensure data integrity and consistency.

To refine the measured data, filtering techniques are applied to reduce noise and outliers, extracting relevant information. Various filtering methods like low-pass filters, high-pass filters, median filters, and Digital Signal Processing (DSP) filters can be used based on requirements.

Once filtered, the data is stored for future analysis. Efficient and scalable storage solutions are crucial to accommodate increasing data volumes while maintaining data integrity. Factors like size, portability, and data transfer speeds must be considered when selecting a storage method. A robust storage system allows for large-scale analysis of short-term and long-term indicators and trends in the data.

By implementing a systematic data processing methodology, users can effectively filter, store, and analyze vast amounts of sensor-generated data. This subsystem explores the intricacies of each processing step, emphasizing design principles and considerations that support an efficient and effective data processing structure. Functional testing of available options for specific steps allows for result compilation and conclusions regarding the system's suitability in addressing the user's problem.

5.2 Design Process & Design Choices

5.2.1 Design Process

Functional Requirements

FR-1 Data measurements should only be taken when a bird is present on the scale.

FR-2 All data measurements must be timestamped.

FR-3 Images of each bird need to correlate with the relevant weight measurements.

FR-4 The system must be able to record the weights of two birds on the scale at the same time. The recording for each those points must be produced individually and a picture needs to be taken of each bird.

FR-5 Data points should be taken for at least each second the bird spends perched on the scale.

FR-6 Final weight value after filtering should be accurate an weight of the bird.

FR-7 The images and data measurements should both be stored in a format that is compatible with a laptop computer.

Non-functional Requirements

NFR-1 Cost of implementation should not exceed R250.00.

NFR-2 The storage device should not run out of storage space.

Functional Specifications

Requirement No.	Functional Specification	Acceptance Criteria
FR-1	FS-1: The data is only recorded when the weight on the scale is non-zero.	The recordings are only taken when the weight on the scale is above a non-zero threshold value.
FR-2	FS-2: The data readings are all recorded along with the time at which they were measured.	The time at which the bird lands on the scale is stored along its weight.
FR-3	FS-3: The image and data point measurements need to correlate. The number of images taken must be the same as the number of weight readings measured.	For each weight reading there is a corresponding image. The image correlates to the data file consistently without failure.
FR-4	FS-4: The scale must be able to account for the weight of each bird individually at all times, even if there are two birds on the scale at the same time.	The final recorded value must be the same for the first whether or not a second bird perches on the scale.
FR-5	FS-5: The frequency of the act of reading values from the scale must be greater than 1 Hz. In other words, the weight value on the scale must be read in more than once a second.	When the threshold is met, frequency of measured weight readings is greater than 1Hz.
FR-6	FS-6: The final weight value after filtering of the recordings must be accurate to the true weight with an accuracy of ± 100 grams.	The final recorded value measured after filtering must be within 100 grams of the true weight placed on the scale.
FR-7	FS-7: The images must be stored in a '.jpg' or '.jpeg' image file format and the data readings from the scale and temperature sensors must be stored in '.txt' text file format.	Image files in '.jpg' or '.jpeg' format and weight and temperature reading files in '.txt' format when stored.

Table 5.1: Table showing the specifications and acceptance criteria for the design of the system.

Requirement No.	Non-functional Specification	Acceptance Criteria
NFR-1	NFS-1: The cost of the hardware required for the storage of the measurement files must be below R250.00.	Total amount in bill of materials relating to the storage of the data should be less than R250.00.
NFR-2	NFS-2: The number of images required to be stored must accommodate an image being taken every minute while in the active power mode.	The SD card can store at least 2000 150KB images.

Table 5.2: Table showing the non-functional specification and its acceptance criteria.

Non-functional Specifications

System Analysis

The stakeholders currently employ a system where the values measured on an analogue scale are read using binoculars, and then the weight along with the corresponding time is manually recorded on a spreadsheet. Simultaneously, bird images are captured using a Browning Elite HP4 camera trap. Since there is a surplus of bird images compared to the number of weight measurements, the timestamps of the images and recorded readings need to be correlated manually.

Unfortunately, the existing system encounters issues leading to inaccurate measurements and unusable data points. For instance, situations arise where a bird swiftly passes by the scale, triggering the camera trap but lacking a corresponding weight reading. Similarly, if a bird remains on the scale for an extended duration, multiple images may correlate to the same weight measurement.

The weight measurement and bird photography processes occur simultaneously but are mutually exclusive, allowing for possible discrepancies in the number of readings between weight measurements and images.

Concept Generation

The data processing system of the project encompasses various aspects where performance plays a crucial role in its overall functionality. However, data acquisition is not among the critical areas. It refers to the method used to retrieve readings from the weight sensors for weight measurement or the temperature sensor for recording environmental temperature during reading. Although some microcontroller boards lack a Real-Time Clock (RTC), an alternative approach involves using the system clock to estimate the reading time based on the duration since the system was powered by the battery.

The pre-processing of the sensor data did not receive detailed attention regarding the available options for capturing the data, as the time difference resulting from using multiple methods was relatively small compared to the computation time of the rest of the system.

Filtering the data required research and analysis of suitable options within the time constraints of the system. The filtering method had to consider the nature of the data, which consisted of unrounded values ranging from two to eight kilograms. The ideal filtering method would analyze both the data values and their surrounding data points. The most effective filtering options with minimal computation requirements include the floating-point filter, low-pass filter, band-pass filter, and mean filter.

Storing the processed data necessitates capturing it without the risk of running out of storage space. Therefore, the storage size for data files and image files should be in the gigabyte range. Suitable

options within this range include SD cards and USB flash drives. The chosen storage device must fit within the system and interface properly with the data processing system. Additionally, it should be capable of withstanding the extreme temperatures experienced by the system, which can reach above 45 degrees Celsius.

Evaluation & Selection

The Arduino Mega 2560 does not have a built-in RTC, and therefore the timestamps of the data values needs to be done in another method. The options available are: using the system clock, using an external RTC, or using internet time synchronisation. The table below illustrates a detailed comparison of the available methods of time stamping.

Timestamp method	Description	Requirements
System clock	The <code>millis()</code> function returns the number of milliseconds that have passed since the Arduino board started or last rest. The timestamps can be created checking the elapsed time and using that as a relative timestamp.	No additional requirements.
External RTC	Connect an external RTC module to the Arduino to provide the system with an accurate timekeeping. Using communication protocols, the time can be retrieved from the RTC module in order to accurately timestamp the measurements.	External RTC module, I2C communication lines, and appropriate library of files are required.
Internet time synchronisation	Can use protocols such as Network Time Protocol (NTP) to retrieve current time from an NTP server.	Access to internet, Wi-Fi module, appropriate libraries of files are required.

Table 5.3: Table showing a comparison of the available options that allow for time stamping of the data recordings.

The filtering of the data readings from the sensors is made up of two parts: the filtering data points based on their values and positions.

The table presented below illustrates the distinctions among several methods that were evaluated during the design process to determine the most suitable filtering approach based on the measurements obtained. Each method's compatibility with a specific type of filtering, aligned with the desired outcomes, is highlighted.

Filtering method	Description	Type of filtering
Floating-point	It allows for precise filtering and manipulation of decimal values. Includes the use of rounding, truncation or threshold-based filtering to exclude or modify data points based on their values.	Value-based filtering.
Low-pass	This filter type preserves low-frequency components. Can be used to smooth out data and reduce noise interference. Examples of low-pass filter implementations are moving average filters or Gaussian filters.	Value-based and position-based filtering.
Band-pass	It allows for isolating or extracting data points that will fall within desired frequency band while suppressing those outside the band.	Value-based filtering.
Mean value	Each data point is replaced with the mean value of its neighbouring data points. It helps to reduce the random variations in the dataset while preserving the overall behavior.	Position-based filtering.

Table 5.4: Table showing a comparison of the different available methods of filtering.

The last aspect of the data processing system that required a design decision was the method of storage for the data points and the supporting images. The images taken on the ESP32CAM are an average of 150KB, as measured from a sample of twenty images. The capacity of the device chosen will be 16GB

in order to accommodate the number of images that need storing. The table below shows the two best suited storage methods that could be implemented in this system.

Storage method	Description	Environmental suitability
USB flash drive	A flash drive is a portable storage device that makes use of flash memory. The use of a USB connection allows for convenient data storage and transfer.	These drives are susceptible to damage from water or dust or physical impact. They are not designed to be waterproof or shockproof.
SD card	Secure Digital (SD) card is a solid-state memory card used for data storage in portable devices. They provide a reliable and removable storage for transferring data between devices.	SD cards are durable and resistant to environmental factors. They are designed to withstand extreme temperatures, shock and water exposure.

Table 5.5: Table showing the comparison between two suitable data storage methods for the system.

5.2.2 Design Choices

There are three design choices that were made in the data processing subsystem, namely: the time stamping of the data readings, method of filtering the data set once all the recordings for a specific bird have been taken, and the method of storage for the data and image files.

The time stamping of the data will be conducted using the system check method described in Table 5.3. This method, based on the *millis()* function, provides a time relative to the program's start rather than real-time accuracy. However, it eliminates the need for an additional module to interface with the Arduino, avoiding unnecessary computational expenses that could impact performance.

The removal of spurious noise from the weight readings of individual birds will be achieved through the implementation of a low-pass filter as can be seen in Table 5.4. In this case, a moving average filter will be employed. The moving average filter effectively filters the data sets by considering both position-based and value-based factors.

When evaluating storage methods for the subsystem, their suitability in different environmental conditions was a crucial factor. Table 5.3 provides a comparison of the considered storage methods. The SD card emerged as a more favorable choice for deployment in the harsh climate of the Kruger National Park. It offers advantages such as a wider effective operating temperature range and better shock resistance, which is particularly relevant considering the potential aggressive behavior of the Southern Ground Hornbills towards the enclosure housing the SD card and its connections. Based on the above choice of storage method, the camera module used in this project will be the ESP32CAM which allows for the process of capturing the image to run simultaneously with the data filtering due to the addition of an additional processor into the system in the form of that ESP32CAM [37].

5.2.3 Acceptance Test Procedures

From the specifications drawn up for this subsystem, tests need to be conducted in order to test the functionality according to what is required. Table 5.6 defines the Acceptance Test Procedure (ATP) for each of the specifications in Table 5.1.

Specification No.	Acceptance Test Procedure	Acceptance Criteria
FS-1	ATP-1: Note the time at which the object was placed on the scale relative to powering on and compare to the start time recorded by the system.	The recordings are only taken when the weight on the scale is above a non-zero threshold value.
FS-2	ATP-2: Note the time at which an object was placed on the scale. Verify weight and time values with a measured time value and an object of known weight.	The time at which the bird lands on the scale is stored along its weight.
FS-3	ATP-3: Place and remove the object multiple times within one run cycle. Verify the number of data readings is accurate and that it matches the number of images.	For each weight reading there is a corresponding image. The image correlates to the data file consistently without failure.
FS-4	ATP-4: Perform a test by placing an object of known weight on the scale, followed by another test where the same object is placed on the scale along with an additional object, running both tests simultaneously for the same duration, and then compare the final values written to the file for both tests.	The final recorded value must be the same for the first bird whether or not a second bird perches on the scale.
FS-5	ATP-5: Conduct a test for a specified duration and verify that the number of readings utilized to calculate the final weight value exceeds the number of seconds in the measured time period.	When the threshold is met, frequency of measured weight readings is greater than 1Hz.
FS-6	ATP-6: Perform a test using an object of known weight while introducing noise while the weight is applied. Confirm that the value written to the file for this object is within 100 grams of true value.	The final recorded value measured after filtering must be within 100 grams of the true weight placed on the scale.
FS-7	ATP-7: After the performing of a test, connect the storage device to a computer to confirm the format produced by the file writing of the weights and images.	Image files in '.jpg' or '.jpeg' format and weight and temperature reading files in '.txt' format when stored.
NFS-1	ATP-8: Calculate the cost of the bill of materials for the components required for the storage of files.	Total amount in bill of materials relating to the storage of the data should be less than R250.00.
NFS-2	ATP-9: Determine maximum available storage for images or data files on the SD card.	SD Card can store at least 2000 images.

Table 5.6: Table showing the ATPs and acceptance criteria for the design of the system.

5.3 Final Design

5.3.1 Data Acquisition

Reading the data from the weight and temperature sensors occurs when the value measured on the scale is above a pre-defined threshold of 2 kg. The weight readings are only recorded for as long as the weight measured on the scale remains above the threshold. The weight readings are measured as well as the temperature at the moment the weight is recorded.

The code snippet in Figure 5.1 shows the functions required to interface with the temperature sensor in order to retrieve the value in degrees Celsius [38]. The code shown makes use of one data pin connection on the Arduino which allows for the transfer of the temperature reading.

```

9  void setup(void)
10 {
11     sensors.begin(); // Start up the library
12 }
13
14 void loop(void)
15 {
16     sensors.requestTemperatures(); // Send the command to get temperatures
17     float temp = sensors.getTempCByIndex(0);
18 }

```

Figure 5.1: Code snippet showing the functions used to interface with the temperature sensor.

The code shown in Figure 5.2 enables the activation of two weight sensors, which are summed to obtain the weight measured on the scale [39]. To convert the measured values from pounds to kilograms, a decimal value is multiplied by each cell's readings. Each weight sensor utilizes a Data Output pin and

a Clock pin on the Arduino. The *get_units()* function returns the measured value on the weight sensor after accounting for the offset introduced by the *tare()* function, and then divides it by the calibration factor to generate an accurate reading.

```

11 float calibration_factor = -91000; //Change this for calibration your load cell
12
13 void setup() {
14     scale.begin(DOUT1, CLK1);
15     scale.set_scale();
16     scale.tare(); //Reset the scale to 0
17
18     scale1.begin(DOUT2, CLK2);
19     scale1.set_scale();
20     scale1.tare(); //Reset the scale to 0
21 }
22
23 void loop() {
24     scale.set_scale(calibration_factor); //Adjust to this calibration factor
25     scale1.set_scale(calibration_factor); //Adjust to this calibration factor
26
27     float sum = abs(scale.get_units()) * 0.453592 + abs(scale1.get_units()) * 0.453592;
28 }

```

Figure 5.2: Code snippet showing the functions used to interact with the weight sensors.

5.3.2 Pre-processing

Capturing of the weight and temperature values measured in data acquisition makes use of an array for bird being measured. The data reading polled from the two weight sensors was tested against an initial threshold to determine if the scale should function as if a bird is present. The reading is then put through a series of if statements to compare its value to a second threshold used to determine if another bird is present on the scale simultaneously.

The two thresholds are set at 2 kg and 6.2 kg. With these thresholds, there are uncertainties within the accuracy of the data readings, but they are based on the common weights of the Southern Ground Hornbills in the Kruger National Park region of a maximum of 4 kg for a female bird and 6 kg for a male.

Figure 5.3 shows the code used to check the value against the thresholds in order to determine where it should be stored as well as if other processes require execution.

5.3.3 Filtering

The moving average filter applied to the arrays holding the readings for each bird can be seen in Figure 5.4. This filter takes in a pointer to the array holding the weight values along with an integer which indicates the number of weight readings that have been recorded and the size of the window used to conduct the calculations.

5.3.4 Storage

The use of an SD card allows for the storage of the data files to be independent of the image file storage, allowing for independent and simultaneous data and image storage on the Arduino and the ESP32CAM [40]. The data values are written to files to be stored on the SD card as can be seen in Figure 5.5.

```

95 //reads values and stores into array depending on number of birds on scale
96 while (totalScaleValue > wakeUpThreshold) {
97     if (bufferIndex1 < 200 && bufferIndex2 < 200) {
98         if (bufferIndex1 == 0) { //first reading of bird 1
99             startTime1 = millis();
100             takePic();
101             sampleBuffer1[bufferIndex1++] = totalScaleValue;
102         } else if ((totalScaleValue < secondBirdThreshold)) {
103             sampleBuffer1[bufferIndex1++] = totalScaleValue;
104         } else if (totalScaleValue >= secondBirdThreshold) {
105             if (numBirds == 0) { //first reading of bird 2
106                 startTime2 = millis();
107                 takePic();
108                 numBirds++;
109             }
110             sampleBuffer2[bufferIndex2++] = totalScaleValue;
111         } else if (totalScaleValue < (sampleBuffer2[bufferIndex2 - 1] - wakeUpThreshold)) {
112             break;
113         }
114     }
115     readScaleVals();
116 }

```

Figure 5.3: Code snippet showing the if statements used to determine the correct array in which to store the data.

```

163 void movingAvgFilter(float* values, int bufferUsed, int windowSize) {
164     float window[windowSize]; // Window to hold the last few values
165     float sum = 0;           // Sum of the values in the window
166
167     // Initialize the window
168     for (int i = 0; i < windowSize; i++) {
169         window[i] = values[i];
170         sum += values[i];
171     }
172
173     // Apply the moving average filter
174     for (int i = windowSize; i < bufferUsed; i++) {
175         values[i] = sum / windowSize; // Update the current array element with the average
176
177         sum -= window[i - windowSize]; // Remove the oldest value from the sum
178         for (int j = 0; j < windowSize - 1; j++) {
179             window[j] = window[j + 1]; // Shift the window values
180         }
181
182         window[windowSize - 1] = values[i]; // Add the newest value to the window
183         sum += values[i]; // Add the newest value to the sum
184     }
185 }

```

Figure 5.4: Code snippet showing the moving average filter applied to the data set.

Each data reading is accompanied by the concurrent temperature measurement. When writing data to a file, the responsible function takes inputs including the initial measurement time, the mean value obtained after filtering, and the temperature. Furthermore, the function calculates and incorporates the confidence interval of the temperature within the recorded weight readings.

```
187 void writeToFile(float meanVal, int startT, float tempVal) {  
188     myFile = SD.open("/data" + String(dataNumber++) + ".txt", FILE_WRITE);  
189  
190     if (myFile) {  
191         myFile.print(startT);  
192         myFile.print(";");  
193         myFile.print(meanVal);  
194         myFile.print(";");  
195         myFile.print(tempVal);  
196         myFile.print(";");  
197         myFile.println(tempVal / 10 * 0.0005 * 20 * 100);  
198     }  
199     myFile.close();  
200 }  
201 }
```

Figure 5.5: Code snippet showing the code to write the data point to the text file.

5.4 Testing & Results

ATP No.	Acceptance Test Procedure	Acceptance Criteria	Test Result
ATP-1	Note the time at which the object was placed on the scale relative to powering on and compare to the start time recorded by the system.	The recordings are only taken when the weight on the scale is above a non-zero threshold value.	Time measured using a stopwatch was equivalent to the time value recorded in the data file. No readings were recorded when weights below the threshold were applied. This ATP is passed.
ATP-2	Note the time at which an object was placed on the scale. Verify weight and time values with a measured time value and an object of known weight.	The time at which the bird lands on the scale is stored along its weight.	By measuring time using a stopwatch and a 2.5 kg weight, the system records readings that align with the known and physically measured results. This ATP is passed.
ATP-3	Place and remove the object multiple times within one run cycle. Verify the number of data readings is accurate and that it matches the number of images.	For each weight reading there is a corresponding image. The image correlates to the data file consistently without failure.	Five readings were recorded as a result of placing and removing the object five times. The number of images captured is also five. This ATP is passed.
ATP-4	Perform a test by placing an object of known weight on the scale, followed by another test where the same object is placed on the scale along with an additional object, running both tests simultaneously for the same duration, and then compare the final values written to the file for both tests.	The final recorded value must be the same for the first bird whether or not a second bird perches on the scale.	For the first object, the final value written to the data file differed by a value of 0.03kg between the two tests. The number of data points recorded in each of the tests was equal. This ATP is passed.
ATP-5	Conduct a test for a specified duration and verify that the number of readings utilized to calculate the final weight value exceeds the number of seconds in the measured time period.	When the threshold is met, frequency of measured weight readings is greater than 1 Hz.	Over a period of 10 seconds, 32 readings were measured. The resulting frequency of measurement is 3.2 Hz. This ATP is passed.
ATP-6	Perform a test using an object of known weight while introducing noise while the weight is applied. Confirm that the value written to the file for this object is within 100 grams of true value.	The final recorded value measured after filtering must be within 100 grams of the true weight placed on the scale.	While the object was on the scale, weight was added and removed through the force of a hand on the scale. The final weight value written to the file aligned with the weight value of the known object measured with no added noise. This ATP is passed.
ATP-7	After the performing of a test, connect the storage device to a computer to confirm the format produced by the file writing of the weights and images.	Image files in '.jpg' or '.jpeg' format and weight and temperature reading files in '.txt' format when stored.	The connection of the SD card to the computer showed the data files in a '.txt' format and the image files in a '.jpg' format. Both files were uncorrupted and accessible on the computer. This ATP is passed.
ATP-8	Calculate the cost of the bill of materials for the components required for the storage of files.	Total amount in bill of materials relating to the storage of the data should be less than R250.00.	The cost for this subsystem totaled R173.00 which is below the limit set of R250.00. This ATP is passed.
ATP-9	Determine the maximum number of images that can be stored on a 16GB SD card.	SD Card can store at least 2000 images to accommodate an image being captured every minute during the active power mode.	The SD card can store 100 000 150KB images which is much larger than the minimum requirement. This ATP is passed.

Table 5.7: Table showing the Acceptance Test Procedures, Acceptance Criteria and test results for the Data Processing subsystem.

The tests determined in Figure 5.6 can all be tested in order to define the performance of the system overall based on its functionality and accuracy. The results of the tests are shown in Figure 5.6.

The testing involved modifying the additional weight applied to the system while the initial object was already on the scale, as depicted in Figure 5.6. These modifications resulted in a marginal alteration in the weight compared to the reading displayed on the scale.

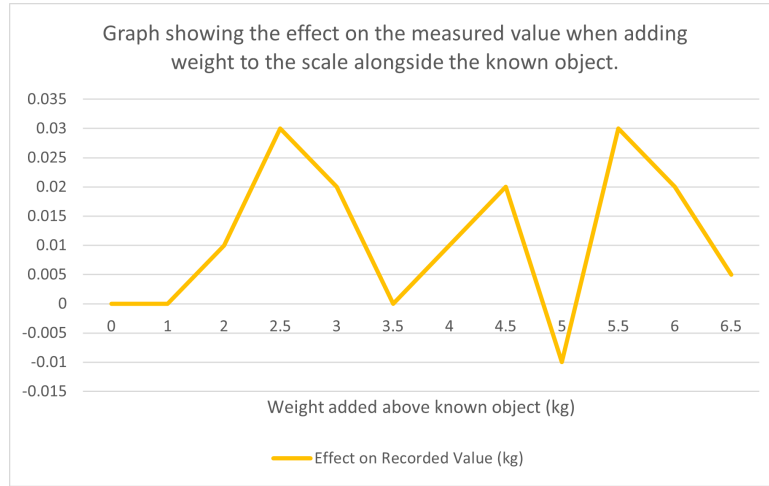


Figure 5.6: Graph showing the relationship between the added weight on the scale and its effect on the recorded value.

The recorded number of readings varied for different durations of weight application on the scale, ranging from 5 seconds to 45 seconds. Figure 5.7 illustrates the relationship between the number of readings and the computation time. Notably, the slope of the number of readings is steeper compared to that of the computation time, suggesting that the computation time is not significantly influenced by the number of readings within this range of values.

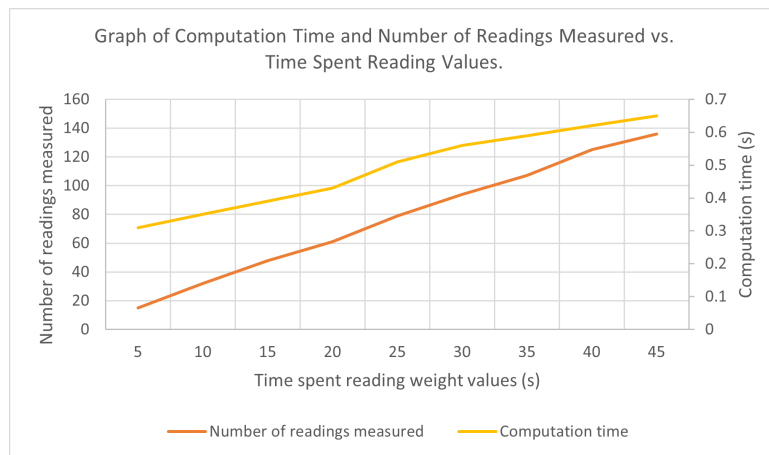


Figure 5.7: Graph showing the relationship between the computation time and number of measured readings and the time spent reading values.

A python script was written for use on a computer which takes correlates the images and data files stored in separate folders and produces a single text file with the data readings along with the relevant image name. This is shown in Figure 5.8.

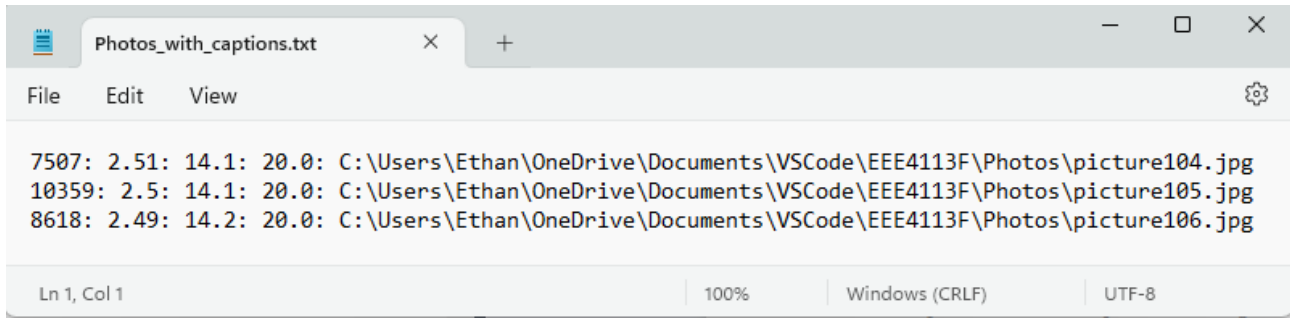


Figure 5.8: Graph showing the relationship between the computation time and number of measured readings and the time spent reading values.

5.5 Conclusion

The requirements and specifications were derived from stakeholder and subsystem needs. Design Process specifications facilitated the creation of Acceptance Test Procedures (ATPs) to assess the design's functionality.

An analysis of the existing system identified the need for an automated solution to record and filter measurements. A Python script was developed to compile and correlate images with data.

The data processing system consists of four stages: reading values from weight and temperature sensors, organizing data based on bird presence, applying a moving average filter to weight readings, and storing filtered weight values with corresponding timestamps and environmental temperature.

ATPs confirmed that the system met all requirements, fulfilling both functional and non-functional specifications.

Based on project findings, recommendations for improvement include implementing an external RTC module for accurate timestamp correlation and exploring alternative filtering methods to handle outliers and noise.

The system's measurement frequency exceeds specifications, allowing for additional filtering methods to be implemented.

Adapting the storage method to incorporate a WiFi module would enable storing files on a web server or online database, facilitating centralized storage of images and data.

Chapter 6

Power Subsystem

6.1 Introduction

In this project, we made specific design choices to ensure an efficient, safe, and simple power model for our autonomous camera trap and weighing system. The initial design incorporated a solar-powered system with a battery backup, utilizing a solar charger controller to manage power sources efficiently. However, considering the territorial and destructive nature of Southern ground hornbills in the area, we decided to opt for a battery-powered setup to avoid potential damage to the solar panels and controller. This section provides an overview of the design choices made, highlighting the selected batteries, buck converters, and solar-based system components. We also determine how long the batteries would last using a power budget.

6.2 Design Choices

The following diagram shows the initial design. We had decided to use a solar powered system, which would power the system when the battery is being recharged. The controller automatically switches power source between the battery and solar panels depending on the power status of the battery. The threshold can also be adjusted to select a different battery level which will trigger the charging mode.

6.2.1 Batteries

LC18650-HT

The LC18650-HT [41] battery is a 3.7V, 2200mAh lithium-ion rechargeable battery. It is a high-top battery, which means that the positive terminal is located at the top of the cell. This type of battery is commonly used in power tools, flashlights, and other portable devices. The battery has several features

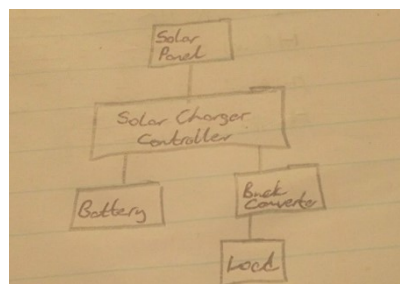


Figure 6.1: Initial Design

that make it a good choice for these applications. It has a high discharge rate, which means that it can provide a lot of power quickly. It also has a long life and can be recharged hundreds of times.

The LC18650-HT battery is a safe and reliable battery. It is protected against overcharging, over-discharging, and short-circuiting. It also has a built-in protection circuit that prevents the battery from being damaged if it is used improperly. The battery is a good choice for a variety of applications. It is a high-quality battery that offers a long life and a high discharge rate. It is also safe and reliable, making it a good choice for power tools, flashlights, and other portable devices.

Here are some additional details about the LC18650 battery [41]:

- Electro-chemical system: Lithium-ion
- Nominal voltage: 3.7V
- Nominal capacity: 2200mAh
- Size: L=66 x D=18.2mm
- Rechargeable: True

EL-12V7AH BATTERIES

EL-12V7AH batteries [42] are 12-volt, 7-amp-hour sealed lead-acid batteries. They are deep-cycle batteries, which means that they can be discharged and recharged many times without losing their capacity. This type of battery is commonly used in solar panels, alarm systems, and other applications where a reliable source of power is needed. EL-12V7AH batteries have several features that make them a good choice for these applications. They have a high discharge rate, which means that they can provide a lot of power quickly. They also have a long life and can be recharged hundreds of times.

Acid batteries are safe and reliable batteries. They are protected against overcharging, over-discharging, and short-circuiting. They also have a built-in protection circuit that prevents the battery from being damaged if it is used improperly. EL-12V7AH batteries are a good choice for a variety of applications. They are a high-quality battery that offers a long life and a high discharge rate. They are also safe and reliable, making them a good choice for solar panels, alarm systems, and other portable devices.

Here are some additional details about the [42] battery:

- Electro-chemical system: Lead-acid
- Nominal voltage: 12V
- Nominal capacity: 7Ah
- Size: L=178 x W=95 x H=100mm
- Weight: 3.5kg
- Rechargeable: True

6.2.2 Buck Converters

LM2596 DC-DC

The LM2596 is a DC-DC converter that is commonly used to step down (buck) the voltage of a power supply. It is a monolithic integrated circuit (IC) that contains all the active components required for a switching regulator. The LM2596 is available in a variety of packages, including TO-220, TO-263, and SMD.

The converter has a number of features that make it a popular choice for DC-DC conversion. It ([43]) can deliver up to 3A of output current, and it has a wide input voltage range of 4.5V to 40V. The LM2596 also has a low dropout voltage ($<1V$), which means that it can be used to efficiently step down a high input voltage to a lower output voltage.

The LM2596 is a versatile DC-DC converter that can be used in a variety of applications. It is commonly used in power supplies for electronic devices, such as routers, switches, and amplifiers. The LM2596 can also be used to power LED lights, motors, and other devices that require a regulated voltage.

Here are some additional details about the [43] DC-DC converter:

- Input voltage range: 4.5V to 40V
- Output voltage range: 1.25V to 35V
- Output current: 3A
- Dropout voltage: $<1V$
- Package options: TO-220, TO-263, SMD

HKD BUCK MODULE LM317T

The HKD Buck Module LM317T is a small, easy-to-use DC-DC converter that can be used to step down (or reduce) the voltage from a higher input voltage to a lower output voltage. It is a popular choice for hobbyists and electronics enthusiasts because it is inexpensive and can be used in a wide variety of applications.

The HKD Buck Module LM317T is based on the LM317 linear regulator, which is an immensely popular voltage regulator that has been used in a wide variety of electronic applications for many years. The LM317 is a three-terminal regulator, which means that it has three connections: an input, an output, and a ground. The input connection is connected to the higher voltage source, the output connection is connected to the load that you want to power, and the ground connection is connected to the negative terminal of the input voltage source.

The HKD Buck Module LM317T works by using the LM317 regulator to control the current that flows through a switching transistor. The switching transistor is turned on and off very quickly by a control circuit. When the switching transistor is turned on, current flows through the transistor and through the load. When the switching transistor is turned off, current stops flowing through the transistor and through the load.

The switching transistor is turned on and off very quickly, so that the average current that flows through the load is less than the current that would flow through the load if the switching transistor was always turned on. This allows the HKD Buck Module LM317T to step down the voltage from the input voltage to the output voltage.

The HKD Buck Module LM317T has a number of features that make it a versatile and useful component for a wide variety of electronic applications. These features include [44]:

- A wide input voltage range: The HKD Buck Module LM317T can be used with input voltages from 4.2 volts to 40 volts.
- A wide output voltage range: The HKD Buck Module LM317T can be used to produce output

voltages from 1.2 volts to 37 volts.

- A high output current: The HKD Buck Module LM317T can provide an output current of up to 1.5 amps.
- A small size: The HKD Buck Module LM317T is a very small component, measuring only 35.6mm x 16.8mm.
- A low cost: The HKD Buck Module LM317T is a very affordable component, making it a smart choice for budget-minded projects.

6.2.3 Solar-Based System Components

SOLAR CHARGER CONTROLLER

A solar charger controller is a device that regulates the charging of a battery using solar energy. It is used in solar power systems to ensure that the battery is charged properly and efficiently.

Solar charger controllers come in a variety of sizes and styles, but they all have the same basic function. They use a series of electronic components to monitor the voltage and current of the battery and the solar panel. The controller then adjusts the amount of current that flows from the solar panel to the battery to ensure that the battery is not overcharged or undercharged.

There are two main types of solar charger controllers: PWM (Pulse Width Modulation) and MPPT (Maximum Power Point Tracking). PWM controllers are the most common type of solar charger controller. They work by turning the solar panel on and off very quickly in a series of pulses. The length of each pulse is determined by the voltage of the battery. This allows the controller to regulate the amount of current that flows from the solar panel to the battery.

MPPT controllers are more expensive than PWM controllers, but they are also more efficient. MPPT controllers work by tracking the maximum power point of the solar panel. The maximum power point is the point at which the solar panel produces the most power. The controller then adjusts the voltage of the battery to match the voltage of the solar panel at the maximum power point. This allows the controller to extract more power from the solar panel and charge the battery more efficiently.

Solar charger controllers are an essential component of any solar power system. They help to ensure that the battery is charged properly and efficiently. This can prolong the life of the battery and improve the performance of the solar power system.

Here are some of the benefits of using a solar [45] controller:

- Prolongs the life of the battery: A solar charger controller helps to prevent the battery from being overcharged or undercharged. This can prolong the life of the battery by up to 50
- Improves the performance of the solar power system: A solar charger controller helps to extract more power from the solar panel. This can improve the performance of the solar power system by up to 20
- Protects the battery from damage: A solar charger controller protects the battery from damage caused by overcharging or undercharging. This can save you money on replacement batteries.
- Extends the warranty of the battery: Many battery manufacturers offer a longer warranty on batteries that are used with a solar charger controller. This can save you money on battery replacements.

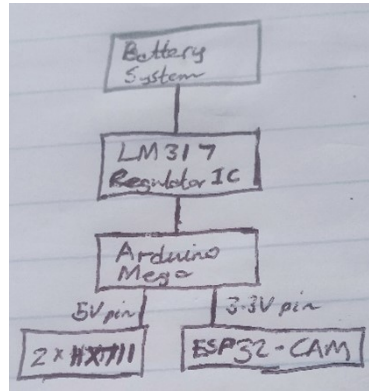


Figure 6.2: Final Design

10W GROWCOL SOLAR PANEL

This panel is small and compact, making it easy to transport and use on the go. It is also lightweight, weighing just 1 kilogram.

The 10W Growcol solar panel [46] is made with high-efficiency monocrystalline solar cells. These cells can convert sunlight into electricity with a conversion efficiency of up to 23

The 10W Growcol solar panel comes with a built-in blocking diode to prevent reverse current flow. This diode helps to protect the panel from damage and ensures that it operates properly. The panel also has a durable aluminium frame that can withstand harsh weather conditions.

The 10W Growcol solar panel is easy to install. It can be mounted on a variety of surfaces, including walls, roofs, and RVs. It is also lightweight and portable, making it easy to transport and use on the go.

The 10W Growcol solar panel is a great option for people who are looking for a small, efficient, and portable solar panel. It is perfect for a variety of off-grid applications, such as camping, RVing, and powering small electronic devices.

There are many benefits to using 10W Growcol solar panels. Some of the most notable benefits include:

- Portability: The 10W Growcol solar panel is lightweight and portable, making it easy to transport and use on the go.
- Efficiency: The 10W Growcol solar panel is made with high-efficiency monocrystalline solar cells that can convert sunlight into electricity with a conversion efficiency of up to 23
- Durability: The 10W Growcol solar panel has a durable aluminium frame that can withstand harsh weather conditions.
- Affordability: The 10W Growcol solar panel is an affordable option for a small, efficient, and portable solar panel.

6.3 FINAL DESIGN

Southern ground hornbills [47] are territorial and notoriously destructive, so they tend to destroy foreign objects which are close to their nesting and perching areas. With this information, we decided to avoid using a solar powered system, since the hornbills would most likely destroy the solar panels, and the solar charger controller would require a large casing, which would catch the attention of the hornbills. The final power setup is shown below:

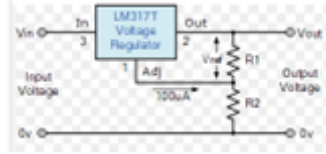


Figure 6.3: LM317 IC

```

151  esp_sleep_enable_ext0_wakeup(GPIO_NUM_13,1);
152
153  Serial.println("Going to sleep now");
154  delay(1000);
155  esp_deep_sleep_start();
156  Serial.println("This will never be printed");

```

Figure 6.4: Sleep mode code for the Arduino Mega

We decided to rely solely on battery power, with the system being driven by two LC18650 batteries. We also bought a charger, as well as two extra batteries for backup. We decided to use the 3V3 and 5V pins on the Arduino to power the camera and the load cell amplifiers.

6.3.1 LM317 Integrated Circuit

The HKD Buck Module we ordered didn't arrive on time, so we had to assemble our own circuit on a perfboard using an LM317, a potentiometer, as well a 2-pin phoenix contact for the battery connection. We managed to get an output voltage of 6.7V from the regulator. The schematic we used to build the circuit is shown below [6.3](#):

6.4 POWER BUDGET

To reduce the system's power consumption, we decided to put all relevant components into sleep mode whenever the system is dormant. Here are some pieces of code we used to implement that [6.4](#).

6.4.1 Active Mode

COMPONENT	CURRENT RATING (mA)	Expected Operation Hours Per Day	Power Consumed Per Day (mAh)
2*HX711	30	5	150
LM317	10	24	150
DS18B20	1.5	5	12
ESP32-CAM	180	0.167	30
10kg Load Cell	5	5	25
Arduino Mega	45	5	225
Total			592

Table 6.1: Power Consumption in Active Mode

6.4.2 Sleep mode

- The power budget has determined that we would have a total power consumption of approximately 719 mAh per day.

COMPONENT	CURRENT RATING (mA)	Expected Operation Hours Per Day	Power Consumed Per Day (mAh)
2*HX711	0.001	19	0.019
LM317	10	0	0
DS18B20	0.001	19	0.019
ESP32-CAM	6	23.833	127
10kg Load Cell	0	19	0
Arduino Mega	0.1	19	1.9
Total			127.632

Table 6.2: Power Consumption in Sleep Mode

- The power capacity of our batteries is 4400 mAh, so the batteries would last about 6 days and 3 hours before they must be recharged. We bought an extra pair so that we could replace the depleted batteries, and the system can still function when they get recharged.

6.5 TESTING/RESULTS

We did not get the opportunity to test how long the batteries would last if the system was continuously in active mode. This was due to most of the components arriving late. However, we did manage to confirm the current and voltage ratings for all the components, and the system works well.

6.6 CONCLUSION

In conclusion, this project aimed to design an efficient, safe, and simple power model for an autonomous camera trap and weighing system. Several design choices were made, considering the various challenges and limitations encountered. Initially, a solar-powered system with a battery backup was planned, but due to the potential damage from the hornbills, a battery-powered setup was chosen instead. The final design utilized two LC18650 batteries, with additional backup batteries and a charger. The system was powered using the 3V3 and 5V pins on the Arduino. An LM317 integrated circuit was used as a buck converter, providing an output voltage of 6.7V.

Although the opportunity to test the system in continuous active mode was not available, the current and voltage ratings were confirmed for all components. Overall, the design choices and power model adopted in this project aimed to address the unique challenges and constraints posed by the environment and wildlife, ensuring the effective operation of the camera trap and weighing system.

Chapter 7

Conclusions

The final system demonstrated successful sensing and storage capabilities during testing. In addition to this, all sub-modules of the automatic scale functioned acceptably upon integration with the microcontroller. The power efficiency of the system was, however, found to be sub-optimal as the device's battery life did not meet the 2 week requirement laid out at the beginning of the design process. Consequently, this submodule requires further improvements. Despite the non-ideal battery life, the project achieved its objective of increasing the accuracy of weight measurements pertaining to SGHs and simplifying the measurement process. Following the implementation of the recommended revisions [8](#) relating to battery life, the end product presents a viable solution to the problems presented by the stakeholders.

Chapter 8

Recommendations

The focus of future revisions would be to minimise the required frequency of site visits. The primary limiting factor of the current design is its battery life. Solar power was considered in the initial designs but after learning of the Southern Ground Hornbills destructive tendencies the idea was discarded to reduce design complexity. In light of the sub-optimal battery life however more of an effort to incorporate autonomous charging should be made in future revisions. Additionally it was noted that the ESP-32 cam draws a significant amount of current and could be removed by directly integrating the camera module into the arduino. This in conjunction with utilising higher capacity batteries would increase the lifespan of the system.

Other improvements regarding the systems enclosure can also be made. Although PLA+ plastic is already more moisture resistant than standard PLA plastic, the resistance to moisture can be increased by coating the enclosure in resin. Alternatively different materials like ABS, PC or metal could be used to form a more durable enclosure. The inclusion of a heatsink in future iterations would allow for the enclosure to passively dissipate heat.

Finally the accuracy of the system can be improved. While the system is already more accurate than manual readings, the start-up calibration could include placing two or more known weights on the scale after taring it in order to determine an accurate calibration factor. This would ensure more consistent results given that the load cells required occasional re-calibration. Finally a camera with better low-light resolution could be used as SGHs typically roost in the early and late hours of the day.

Bibliography

- [1] D. E. Ausband, J. Skrivseth, and M. S. Mitchell, “An automated device for provoking and capturing wildlife calls,” in *Wildlife Society Bulletin*, vol. 35, 2011, pp. 498–503.
- [2] A. L. Borker, P. Halbert, M. W. Mckown, B. R. Tershy, and D. A. Croll, “A comparison of automated and traditional monitoring techniques for marbled murrelets using passive acoustic sensors,” in *Wildl. Soc. Bull.*, vol. 39, 2015, pp. 813–818.
- [3] V. Dyo, S. Ellwood, D. Macdonald, A. Markham, C. Mascolo, B. Pasztor, S. Scellato, N. Trigoni, R. Wohlers, and K. Yousef, “Evolution and sustainability of a wildlife monitoring sensor network,” in *Proceedings of the First ACM Workshop on Embedded Sensing Systems for Energy-Efficiency in Buildings*, 2010, pp. 127–140.
- [4] J. A. Zwerts, P. J. Stephenson, F. Maisels, M. Rowcliffe, C. Astaras, P. A. Jansen, J. van der Waarde, E. Sterck, P. A. Verweij, T. Bruce, S. Brittain, and M. van Kuijk, “Methods for wildlife monitoring in tropical forests: Comparing human observations, camera traps, and passive acoustic sensors,” in *Conservation Science and Practice*, vol. 3, 2021, p. e568.
- [5] F. Trollet, M.-C. Huynen, C. Vermuelen, and C. Humbuckers, “Use of camera traps for wildlife studies. a review,” in *Mammalia*, vol. 78, 2014, pp. 446–454.
- [6] H. Handcock, D. Swain, G. Bishop-Hurley, K. Patison, T. Wark, P. Valencia, P. Corke, and C. O’Neill, “Monitoring animal behaviour and environmental interactions using wireless sensor networks, gps collars and satellite remote sensing,” in *Sensors (Basel)*, vol. 9, 2009, pp. 3586–3603.
- [7] South African National Biodiversity Institute. (2019) Southern ground-hornbill. [Online]. Available: <https://www.sanbi.org/animal-of-the-week/southern-ground-hornbill/>
- [8] A. Kemp and M. Kemp, “The biology of the southern ground hornbill *bucorvus leadbeateri* (vigors) (aves: Bucerotidae),” *Annals of the Transvaal Museum*, vol. 32, no. 4, pp. 65–100, 1980. [Online]. Available: http://hdl.handle.net/10520/AJA00411752_574
- [9] BirdLife South Africa. Southern ground hornbill. [Online]. Available: <https://www.birdlife.org.za/what-we-do/landscape-conservation/what-we-do/large-terrestrial-birds/southern-ground-hornbill/>
- [10] Mabula Ground-Hornbill Project. Conserving the southern ground hornbill. [Online]. Available: <https://ground-hornbill.org.za/>
- [11] J. Gula and C. G. Phiri, “Observations of southern ground-hornbill *Bucorvus leadbeateri* groups in the kafue national park, zambia,” *Ostrich*, vol. 91, no. 3, pp. 267–270, 2020.

- [12] J. Dickens. (2010) How much is enough. [Online]. Available: <https://apnrgroundhornbillsproject.files.wordpress.com/2020/08/dickens-j-2010-calibrating-sattelite-telemetry.pdf>
- [13] N. Theron, R. Jansen, P. Grobler, and A. Kotze, “The home range of a recently established group of southern ground-hornbill (*bucorvus leadbeateri*) in the limpopo valley, south africa,” *Koedoe*, vol. 55, no. 1, pp. 1–8, 2013. [Online]. Available: <https://doi.org/10.4102/koedoe.v55i1.1088>
- [14] Sabi Sabi. Southern ground hornbill project. [Online]. Available: <https://www.sabisabi.com/discover/topics/southern-ground-hornbill-project>
- [15] K. Kerry, J. Knowles, and G. Else, “The use of an automated weighing and recording system for the study of the biology of adélie penguins (*Pygoscelis adeliae*),” in *Proceedings of the NIPR Symposium on Polar Biology*, vol. 6, 1993, pp. 62–75.
- [16] A. Poole and J. Shoukimas, “A scale for weighing birds at habitual perches,” *J. Field Ornithol.*, vol. 53, no. 4, pp. 409–414, 1982.
- [17] K. Wang, J. Pan, X. Rao, Y. Yang, F. Wang, R. Zheng, and Y. Ying, “An image-assisted rod-platform weighing system for weight information sampling of broilers,” *Transactions of the ASABE*, vol. 61, no. 2, pp. 631–640, 2018.
- [18] M. Oswa, R. Zhao, and J. Paul, “Ultralife - india,” May 07 2010. [Online]. Available: https://www.ultralifeindia.com/wp-content/uploads/2020/03/LFP_study.pdf
- [19] H. Bindner, T. Cronin, and P. Lundsager, “Lifetime modelling of lead acid batteries,” in *7th International Conference on Developments in Power System Protection*, 2005. [Online]. Available: <https://ieeexplore.ieee.org/document/1595244>
- [20] J. Marsh. (2022, Dec) Lithium-ion vs. lead acid batteries: How do they compare?: Energysage. [Online]. Available: <https://news.energysage.com/lithium-ion-vs-lead-acid-batteries/>
- [21] S. Ma, M. Jiang, P. Tao, C. Song, J. Wu, J. Wang, T. Deng, and W. Shang, “Temperature effect and thermal impact in lithium-ion batteries: A review,” *Progress in Natural Science: Materials International*, vol. 28, no. 6, pp. 653–666, 2018.
- [22] R. Hutchinson, “Temperature effects on sealed lead acid batteries and charging techniques to prolong cycle life,” 2011. [Online]. Available: [doi:10.2172/975252](https://doi.org/10.2172/975252)
- [23] P. J. Apps and J. W. McNutt, “How camera traps work and how to work them,” *Afr. J. Ecol.*, vol. 56, pp. 702–709, 2018.
- [24] M. Rössler, W. Laube, and P. Weihs, “Avoiding bird collisions with glass surfaces: Experimental investigations of the efficacy of markings on glass panes under natural light conditions in flight tunnel ii,” 2009.
- [25] Mustafa, “How does load cell work?” KOBASTAR Load Cell & Indicator, Nov. 2017, [Accessed May 18, 2023]. [Online]. Available: <https://kobastar.com/en/how-does-a-load-cell-work/>
- [26] eliteio. (2022, November 19) DS18B20. [Online]. Available: <https://github.com/eliteio/DS18B20>

- [27] bogde, “bogde/HX711,” <https://github.com/bogde/HX711>, Mar. 2019, gitHub repository.
- [28] IEC, “Ip ratings,” "<https://www.iec.ch/ip-ratings#:~:text=The%20standard%2C%20prepared%20by%20IEC,the%20enclosure%20meets%20these%20requirements>", [Accessed May 16, 2023].
- [29] R. Poola, “Design considerations for ip-rated telecom products and enclosure,” <https://www.hcltech.com/sites/default/files/documents/design-considerations-for-ip.pdf>, January 2011, [Accessed May 16, 2023].
- [30] RS, “The comprehensive guide to ip ratings,” <https://au.rs-online.com/web/generalDisplay.html?id=ideas-and-advice%2Fip-ratings>, [Accessed May 16, 2023].
- [31] CIE, “What are ik ratings?” <https://cie-group.com/how-to-av/videos-and-blogs/ik-ratings>, [Accessed May 16, 2023].
- [32] RasPi.TV, “How much power does pi zero w use?” <https://raspi.tv/2017/how-much-power-does-pi-zero-w-use>, [Accessed May 18, 2023].
- [33] APNR Southern Ground-Hornbill Research & Conservation Project. Apnr southern ground-hornbill research & conservation project. [Online]. Available: <https://apnrgroundhornbillproject.com/>
- [34] meteoblue, “Simulated historical climate & weather data for kruger national park,” https://www.meteoblue.com/en/weather/historyclimate/climatemodelled/kruger-national-park__south-africa__986833/, [Accessed May 18, 2023].
- [35] C. G. Amza, A. Zapciu, F. Baci, M. I. Vasile, and D. Popescu, “Aging of 3d printed polymers under sterilizing uv-c radiation,” https://www.researchgate.net/publication/357198864_Aging_of_3D_Printed_Polymers_under_Sterilizing_UV-C_Radiation/link/61c57ae8b8305f7c4bf95652/download, [Accessed May 18, 2023].
- [36] F. Arceo, “3d filament glass transition temperatures,” <https://3dsolved.com/3d-filament-glass-transition-temperatures/>, [Accessed May 18, 2023].
- [37] R. N. Tutorials, “Esp32-cam take photo and save to microsd card,” Dec. 10 2019. [Online]. Available: <https://randomnerdtutorials.com/esp32-cam-take-photo-save-microsd-card/>
- [38] —, “Guide for ds18b20 temperature sensor with arduino,” Jul. 02 2019. [Online]. Available: <https://randomnerdtutorials.com/guide-for-ds18b20-temperature-sensor-with-arduino/>
- [39] —, “Arduino with load cell and hx711 amplifier (digital scale),” Apr. 27 2022. [Online]. Available: <https://randomnerdtutorials.com/arduino-load-cell-hx711/>
- [40] —, “Guide to sd card module with arduino,” Sep. 08 2017. [Online]. Available: <https://randomnerdtutorials.com/guide-to-sd-card-module-with-arduino/>
- [41] Communica. (2023) Lc18650-ht. [Online]. Available: <https://www.communica.co.za/products/lc18650-ht>
- [42] Takealot. (2023) 12v 7ah solar battery-acid. [Online]. Available: <https://www.takealot.com/12v-7ah-solar-battery-acid/>

PLID91188245?gad=1&gclid=CjwKCAjwvJyjBhApEiwAWz2nLX7QzHR__fP8pT-XMHlyJFFcBZz0brlOIGJ8yeFNT5cVu05BvXhwliBoC0csQAvD__BwE&gclsrc=aw.ds

- [43] Onsemi. (2023) 3.0 a, step-down switching regulator. [Online]. Available: <https://www.onsemi.com/pdf/datasheet/lm2596-d.pdf>
- [44] Communica. (2023) Hkd dc/dc buck module -lm317t. [Online]. Available: <https://www.communica.co.za/products/hkd-dc-dc-buck-module-lm317t?variant=40083148701769>
- [45] ——. (2023) Vict bluesolar pwml 12-24 5a. [Online]. Available: <https://www.communica.co.za/products/vict-bluesolar-pwml-12-24-5a?variant=43975520289068>
- [46] G. Solar. (2023) Growcol 10w mono. [Online]. Available: <https://onlineshop.gcsolar.co.za/product/growcol-solar-panel-10w/>
- [47] S. D. Z. W. A. Library. (2023) Example website. [Online]. Available: https://ielc.libguides.com/sdzg/factsheets/southern_groundhornbill/behavior